KINETIC STUDY OF Fe(III) ION WITH SOME ISONICOTINOYL HYDRAZONES

BY

SOMRUDEE CHETUPHON (B.Sc. in Chem.)

A THESIS SUBMITTED IN PARTIAL FULFILMENT OF

THE REQUIREMENTS FOR THE DEGREE OF

MASTER OF SCIENCE

(PHYSICAL CHEMISTRY)

IN

THE FACULTY OF GRADUATE STUDIES

OF

MAHIDOL UNIVERSITY

1985

This Thesis

entitled

KINETIC STUDY OF Fe(III) ION

WITH SOME ISONICOTINOYL HYDRAZONES

was submitted to the Faculty of Graduate Studies,

Mahidol University, for the MASTER OF SCIENCE degree

on July 29, 1985

Somrudee Chetuphon

.....

Somrudee Chetuphon

Candidate

Prapin Wilairat

.....

Dr. Prapin Wilairat

Preceptor

Preedeeporn Limcharoen

.....

Dr. Preedeeporn Limcharoen

Copreceptor

Waret Veerasai

.....

Dr. Waret veerasai

Copreceptor

M. Chulasamaya

.....

Dr. Manthree Chulasamaya

Dean, Faculty of Graduate Studies

Mahidol University,

Pairote Prempree

.....

Dr. Pairote Prempree

Dean, Faculty of Science

Mahidol University

EVALUATION OF THE FINAL EXAMINATION

THE DEFENCE OF THESIS

We, the members of the supervisory Graduate Committee

for

SONRUDEE CHETUPHON

unanimously approve the thesis entitled

KINETIC STUDY OF Fe(III) ION

WITH SOME ISONICOTINOYL HYDRAZONES

We further agree that she has satisfactorily defended

her thesis at the examination given by the

supervisory committee

on

July 29, 1985

We recommended therefore that

Somrudee Chetuphon

be awarded the degree of Master of Science in

Physical Chemistry

from

Mahidol University

.....

Dr. Prapin Wilairat

Preceptor

.....

Dr. Preedeeporn Limcharoen

Copreceptor

.....

Dr. Waret veerasai

Copreceptor

.....

Dr. Manthree Chulasamaya

Dean, Faculty of Graduate Studies

Mahidol University

BIOGRAPHY

Name : Somrudee Chetuphon

Date of Birth : October 25, 1958

Place of Birth : Burcerum, Thailand

Institution attended : Satrividhaya School, Bangkok

March, 1977 - Certificate of M.S.5

Mahidol University, Bangkok

March, 1981 - B.Sc. (Chemistry)

ACKNOWLEDGEMENTS

I wish to express my thanks to my advisor, Dr. Prapin Wilairat, for his guidance, suggestions, discussions throughout the research program and finally for his corrections of the manuscript. I also thanks Dr. Preedeeporn Limcharoen and Dr. Waret Veerasai for their valuable comments and acting together as the coprreceptors.

In addition, I wish to thank the kind support of the National Research Council of Thailand, the Department of Chemistry, Mahidol University, for Laboratory facilities and my friends for their help.

Finally, I deeply thank to Mr. Chalermchai Alongkhonrussamee, for his kind support and help through this study.

LIST OF FIGURES

Figure		page
2.1	Calibration curve of observed pH against $[HNO_3]$	24
2.2	Calibration curve of standard ferric nitrate solution	26
3.1	IR-spectrum of PSH	31
3.2	UV-Vis spectra of PSH at various pH	32
3.3	UV-Vis spectra of PSH in MeOH	33
3.4	Absorbance of PSH at various pH	36
3.5	UV-Vis spectra of free PBH, free Fe(III) and Fe(III)-PBH complex at $[H^+]$ = 0.05 M, conc. ca 8×10^{-5} M PBH	39
3.6	UV-Vis spectra of free PBH, free Fe(III) in chloroacetic acid buffer and Fe(III)-PBH complex in chloroacetic acid buffer at $[H^+]$ = 0.05 M, conc. ca 8×10^{-5} M PBH	40
3.7	Value of k_{obsd} as a function of $[Fe^{3+}]_T$ for the reaction of Fe(III)-PBH at various $[H^+]$	41
3.8	Value of k_{obsd} as a function of $[H^+]$ for the reaction of Fe(III)-PBH at various $[Fe^{3+}]_T$	42
3.9	UV-Vis spectra of free PSH, free Fe(III) and Fe(III)-PSH complex at $[H^+]$ = 0.05 M, conc. ca 8×10^{-5} M PSH	45
3.10	Value of k_{obsd} as a function of $[Fe^{3+}]_T$ for the reaction of Fe(III)-PSH at various $[H^+]$	46
3.11	Value of k_{obsd} as a function of $[H^+]$ for the	47

Figure (continued) page

reaction of Fe(III)-PSH at various $[Fe^{3+}]_T$

3.12 Dependence of "b" on $1/[H^+]$ for the reaction of Fe(III)-PBH 52

3.13 Dependence of "b" on $1/[H^+]$ for the reaction of Fe(III)-PSH 53

LIST OF TABLES

Table		page
1	Summary of rate constants ($M^{-1}s^{-1}$) for various Fe(III) path way	16
2.1	pH of various nitric acid concentrations	23
2.2	Calibration curve of standard ferric nitrate solution	25
3.1	Kinetic data for the Fe(III)-PBH system	37
3.2	Kinetic data for the Fe(III)-PSH system	43
3.3	Experimental values of "b" for the Fe(III)-PBH system	51
3.4	Experimental values of "b" for the Fe(III)-PSH system	54
3.5	Summary of rate constant for Fe(III)-PBH and Fe(III)-PSH system	54

TABLE OF CONTENTS

		page
CHAPTER I	GENERAL INTRODUCTION	1
1.1	Solvated Metal Ions	2
1.2	Substitution Reactions of Octahedral Complexes in Aqueous Solution	4
1.3	Kinetics of Replacement of Coordinated Water Involving Multidentate Ligands	6
1.4	Outer-Sphere Association Constant	8
1.5	Factors Giving Rise to Anomalous Rate	10
1.6	Statistical Factor for Id Mechanism	12
1.7	Hydrolysis of Ferric Ion Solution	13
1.8	Aquo-Ligand Complexes of Iron(III) Metal Ion	15
1.9	The Scope of This Thesis	18
CHAPTER II	EXPERIMENTAL SECTION	19
2.1	Abbreviation and Symbols	19
2.2	Chemicals	21
2.3	Spectrophotometers	22
2.4	Thermostating	22
2.5	pH Meter	22
2.6	Preparation and Chemical Analysis of Materials	23
2.7	General Experimental Procedure	27
	2.7.1 pK_a Measurement of Pyridoxal Salicyloyl Hydrazone	27
	2.7.2 Kinetic Measurements	28
2.8	Treatment of Data	29

page

CHAPTER III RESULTS AND MECHANISM 30

3.1 Analytical Properties of Pyridoxal Salicyloyl Hydrazone 30

3.1.1 IR-Spectroscopy 30

3.1.2 UV-Visible Spectroscopy 30

3.2 pH Measurement 34

3.3 Kinetic Measurements 37

3.3.1 Kinetic of Fe(III) Ion and Pyridoxal Benzoyl Hydrazone 37

3.3.2 Kinetic of Fe(III) Ion and Pyridoxal Salicyloyl Hydrazone 43

3.4 Reaction Mechanism 48

CHAPTER IV DISCUSSION 55

SUMMARY 60

APPENDIX 61

REFERENCES 62

CHAPTER ONE

GENERAL INTRODUCTION

In recent years there have been renewed interests in the study of chelating agents for iron (III), with the ultimate goal in mind as drugs for use in iron-overload diseases. The only practical method of iron mobilization in such diseases is the use of iron-chelating drugs, of which the commercially available agent desferroxamine (DF)[1] is distinguished by its lack of significant toxicity. However because of its limited gastrointestinal absorption and its high cost, current interest is focused on the development of new iron-chelating agents that might be better suited for large-scale clinical use.

Since Ponka et al.[2] discovered pyridoxal isonicotinoyl hydrazone as a chelating agent of promise, research has been undertaken to assess the ability of this hydrazone and related compounds to bind iron. Pyridoxal benzoyl hydrazone was found to produce high levels of iron excretion in vivo which exceed that seen with an equivalent dose of desferroxamine B.[3] Pyridoxal salicyloyl hydrazone has been used as a spectrophotometric reagent for determining trace amount of zirconium (IV),[4] aluminium (III)[5]. Investigation of mechanism by kinetic studies will help to understand the detailed progress of reaction, i.e the elementary steps involved and their relative rates in the over all mechanism scheme. This work is to study the kinetics of the reaction of $Fe(H_2O)_6^{3+}$ ion with pyridoxal benzoyl hydrazone and pyridoxal salicyloyl hydrazone.

In order to provide a relevant basis for the kinetic study, the general mechanism of complex formation is presented, and examples are shown.

1.1) Solvated Metal Ion

The reactions of metal complexes in solution are accounted for from the properties of the solvated cation. The information needed to characterise ionic solvation includes the solvation number of the ion, the distance between the ion and adjacent solvent molecules, the strength of ion-solvent interactions, and delocalisation of charge from the ion onto adjacent solvent molecules.

A cation in aqueous solution has a primary solvation shell, containing water molecules directly interacting or bonding with the cation, and region of secondary solvation resulting from the electron-withdrawing effect of the cation on the primary waters of hydration which encourages them to hydrogen-bond to secondary waters of hydration[6,7]. Several methods to determining the solvation number of cation have been reviewed by Burgess[8] (Chapter2-4). These are spectroscopic techniques (nmr- , esr- spectroscopy, UV-Visible spectroscopy, vibrational spectroscopy) non-spectroscopic methods (transport properties, for example transference no., ionic conductance, viscosities, diffusion ; thermochemical approaches eg. entropy, compressibility, volume ; other approaches such as diffraction methods) and isotope dilution techniques. Although there is a range of values for the hydration

number of each cation depending on methods and assumption used, for cation of a given charge, hydration numbers tend to decrease as cation size increases ; for cation of similar size, the hydration number increases greatly as cation charge increases.

The solvent exchange process is generally written as

$$M(Solv)_n^{m+} + {}^*Solv \rightleftharpoons M(Solv)_{n-1}({}^*Solv)^{m+} + Solv \qquad (1.1)$$

If the solution also contains another ligand, solvent in the solvated ion can be replaced. The second ligand may occupy one (unidentate ligand) or more (multidentate ligand) of the solvent positions ; for example, in the simple case of a neutral unidentate ligand ,L, replacing H_2O

$$M(H_2O)_n^{m+} + L \rightleftharpoons M(H_2O)_{n-1}L^{m+} + H_2O \qquad (1.2)$$

leading eventually to

$$M(H_2O)L_{n-1}^{m+} + L \rightleftharpoons ML_n^{m+} + H_2O \qquad (1.3)$$

In order to measure the metal-ligand interactions, the stability constant for eqns. (1.2) and (1.3) is introduced as

$$K_1 = \frac{[M(H_2O)_{n-1}L^{m+}]}{[M(H_2O)_n^{m+}][L]} \qquad (1.4)$$

and $$K_n = \frac{[ML_n^{m+}]}{[M(H_2O)L_{n-1}^{m+}][L]} \qquad (1.5)$$

The value K_1, K_n are often essential and useful in the interpretation of the kinetics of metal complex formation.

1.2) Substitution Reactions of Octahedral Complexes in Aqueous Solution

The basic classification of substitution reactions is into dissociative and associative or unimolecular (S_N1) and bimolecular (S_N2) processes. The use of a slightly more detailed classification can subdivide the range of possible mechanisms into the following four groups ; one is S_N1(lim) or D mechanism, in which a transient intermediate of five-coordination number is generated and persist long enough to discriminate between potential ligands in its vicinity.

$$M(H_2O)_6^{n+} \rightleftharpoons M(H_2O)_5^{n+} + H_2O \qquad k_1, k_{-1} \qquad (1.6)$$

$$\Big\downarrow\uparrow$$

$$M(H_2O)_5L^{(n-m)} \qquad k_2, k_{-2} \qquad (1.7)$$

where k_1, k_2 and k_{-1}, k_{-2} are the forward and backward rate constants respectively.

The second mechanism is the dissociative interchange (Id) mechanism which involve outer-sphere or ion-pair association between the starting complex and ligand. Because of this, the

incoming ligand is suitably placed to enter the primary coordination sphere of the metal ion as soon as the water molecule has left from the inner sphere. For most labile metal ions the rate-determining step is the breaking of $M-OH_2$ bond, not the formation of M-L bond. Therefore, the rates of ligand substitution reactions are described as being controlled by the rate of exchange of water from the inner sphere and are independent of the nature of the incoming ligand.

$$M(H_2O)_6^{n+} + L^{m-} \underset{}{\overset{K_{os}}{\rightleftharpoons}} (H_2O)M(H_2O)_5.L^{(n-m)} \qquad (1.8)$$

$$(H_2O)_5M(H_2O).L^{(n-m)} \underset{k_{-1}}{\overset{k_1}{\rightleftharpoons}} M(H_2O)_5L^{(n-m)} + H_2O \qquad (1.9)$$

This mechanism leads to an observed pseudo-first order rate constant.

$$k_{obsd} \qquad \frac{K_{os}\, k_1 [X] + k_{-1}}{(1+K_{os}[X])} \qquad (1.10)$$

where [X] is the species in excess (i.e pseudo-first order in [X]). In most experiments the concentration of reactants are small so that $K_{os}[X] << 1$. Then the equation (1.10) reduces to

$$k_{obsd} = K_{os}\, k_1 [X] + k_{-1} \qquad (1.11)$$

$$= k_f [X] + k_b \qquad (1.12)$$

Although an interchange dissociative mechanism is favored in large number of reaction of octahedral complexes, evidence for the two mechanisms, the associative ,A, or $S_N2(lim)$ and the interchange associative (Ia) process have been found for selected system. Just as the Id mechanism there is an interchange of ligands between the primary and secondary coordination regions in Ia mechanism. But the main feature in A mechanism is the formation of an intermediate of seven-coordination number.

1.3) Kinetics of Replacement of Coordinated Water Involving Multidentate Ligand

The reaction rates of multidentate ligands with aquometal ions are found to vary more than the rate of monodentate ligands. Considering the bidentate ligands as a general mechanism

$$\underset{(I)}{M(H_2O)_6^{n+}} + (L\text{-}L)^{m-} \underset{}{\overset{K_{os}}{\rightleftharpoons}} (H_2O)_5M(H_2O).(L\text{-}L)^{n-m} \qquad (1.13)$$

$$(H_2O)_5M(H_2O).(L\text{-}L)^{n-m} \underset{k_{-2}}{\overset{k_2}{\rightleftharpoons}} \underset{(II)}{\left[(H_2O)_5M\text{-}L\text{-}L\right]^{n-m}} + H_2O \qquad (1.14)$$

$$\underset{(III)}{\left[(H_2O)_5M\text{-}L\text{-}L\right]^{n-m}} \underset{k_{-3}}{\overset{k_3}{\rightleftharpoons}} \underset{(IV)}{\left[(H_2O)_4\ M\!<\!\begin{matrix}L\\L\end{matrix}\right]^{n-m}} + H_2O \qquad (1.15)$$

where species (II) is an outer-sphere complex, species (III) is mono-coordinated complex and species(IV) is chelated complex.

It is assumed that the diffusion to form the outer-sphere complex is very rapid and that the stationary state

approximation can be applied to the intermediate (species (III)). The rate expression is then given by,

$$k_f = \frac{K_{os} k_2 k_3}{(k_{-2} + k_3)} \qquad (1.16)$$

$$k_b = \frac{k_{-2} k_{-3}}{(k_{-2} + k_3)} \qquad (1.17)$$

For most bidentate ligands, the chelate ring-closure step is much faster than the breaking of the first metal-ligand bond, i.e $k_3 >> k_{-2}$.

$$k_f = K'_{os} k_2 \qquad (1.18)$$

$$k_b = \frac{k_{-2} k_{-3}}{k_3} \qquad (1.19)$$

In this case "normal substitution" is indicated and the bidentate (or multidentate) ligand resembles the appropiate unidentate ligand, for which only the rate of formation of M-L-L entity is meaningful.

For example, the rate constant for the complex formation of $Ni(H_2O)_5py^{2+}$, $Ni(H_2O)_4bipy^{2+}$ and $Ni(H_2O)_3terpy^{2+}$, in which only one Ni-N bond has to form, is very similar[9].

If $k_{-2} >> k_3$ (i.e ring closure is rate determining step),

this is called "sterically controlled substitution" (SCS) process with

$$k_f = \frac{k_3 k_2 K_{os}}{k_{-2}} \qquad (1.20)$$

$$k_b = k_{-3} \qquad (1.21)$$

1.4) Outer-Sphere Association Constant

There are several methods for estimating K_{os}, the outer-sphere association constant. These may emerge as a result of kinetic studies, or they may be obtained directly from spectral, polarimetry, nmr measurement, but only for inert complexes. For labile metal ions K_{os} values are more difficult to determine. Theoretical expressions derived from a consideration of statistical argument by Fuoss[10] and the theory of diffusion by Eigen[11] for calculating the K_{os} value is given by

$$K_{os} = \frac{4\pi N a^2 e^{-b}}{3000} \cdot \exp\left[\frac{b\kappa a}{(1+\kappa a)}\right] \qquad (1.22)$$

where $b = \frac{Z_M Z_L e^2}{a\epsilon kT}$

a = center to center distance (cm) between the species M and L

N = Avogadro's number

Z_M = formal charge on the metal ion

Z_L = formal charge on the ligand

e_o = electric charge (esu)

ϵ = dielectric constant of the solvent

k = Boltzmann constant (erg)

T = absolute temperature (K)

κ = Debye-Hückel ion atmosphere parameter

$\kappa^2 = \dfrac{8\pi Ne^2\mu}{1000\epsilon kT}$

where μ = ionic strength of the solution

The value of K_{os} is sensitive to the choice of a, which varies from one complex to another. The frequently used value of a is 4-5 A^o and gives the simpler expression,

$$K_{os} = \left(\frac{4}{3}\pi a^3 N e^{-b}\right).10^3 \quad mol^{-1}dm^{-3} \qquad (1.23)$$

For cases where a bidentate ligands such as mono-protonated ethylenediamine, enH^+ reacts, Rorabacher et al[12] have modified expression (1.23) to

$$K_{os} = \frac{4}{3}\pi a^3 N \exp\left[\frac{-Z_M Z_L e_o^2}{a'\epsilon kT}\right] \cdot 10^{-3} \quad mol^{-1}dm^{-3} \qquad (1.24)$$

where a,a' = center to center distance between the metal ion and the unprotonated, protonated nitrogen

donor of en respectively

1.5) Factor Giving Rise to Anamalous Rates

1) Steric Effect

In multidentate ligand complex formation, steric effect may become important in the ring-closure step as well as in the initial coordination step. Steric hindrance can be large enough to change the rate-determining step from first- to second-bond formation.

From equation (1.16) and (1.17), if $k_3 << k_{-2}$ then the ring-closure step can be rate-limiting step. Therefore

$$k_f = \frac{K_{os} k_2 k_3}{k_{-2}} \qquad (1.25)$$

and $k_b = k_{-3}$

Comparing the k_f values for the two conditions eqns. (1.18) and (1.25), it is found experimentally that the ring-closure step causes the k_f value to be abnormally slow. For example, the lower rate constant observed for β-alanine (ca. 10X slower) as compared to α-alanine binding with Ni^{2+} and Co^{2+} [13]. Similar steric effects have been reported for the reaction of α- and β-aminobutyrates[14] with Ni^{2+} and α- and β-alanines and histidine with Cu^{2+} [15]. This is thought to be the difficulty in

the forming 6-membered ring compared to a 5-membered ring.

2) Effect of Hydroxide Ion

Most labile metal ions can hydrolyse easily even in the acidic medium. The hydrogen ion in $M(H_2O)_5OH^{m+}$ can modify reactivity of the system. It labilizes the remaining water molecule and thus k_f value increases. The rate constant for water exchange on $Fe(H_2O)_5OH^{2+}$ is very roughly 10^2 times larger than that for water exchange on $Fe(H_2O)_6^{3+}$ [16].

3) Effect of Protonated Ligand

In general, the rates between a metal ion and the protonated form of the ligand are lower than the rates for binding with the basic form. By considering the ratios of k_f values for $H_{n-1}L$ compared with H_nL, it can be seen that two rough cases may be formed. Firstly, the protonation causes a significant decreases in the formation rate, resulting in a k_f ratio for $H_{n-1}L$ to H_nL which is between 10 and 10^3. In this case protonation will have less effect if the rate-determining step occur early in the coordination of the multidentate ligand. Therefore, the decrease in the rate constant is not too great when these bidentate ligand add a proton. Secondly protonation has a greater effect, causing the k_L/k_{HL} ratio to be 10^3 to 10^7. Several factors can cause a large decrease in the formation rate as a result of protonation such as internal conjugate base rate

enhancement, electrostatic repulsion, statistical effect and intramolecular hydrogenbonding.

4) Effect of Buffers

In order to keep the concentration of hydrogen ion constant, a buffer must be employed. The presence of sufficiently high concentration of buffer means that the proton-transfer step occur efficiently via the buffer system, BH and B[17]:

$$L + BH \rightleftharpoons B + LH$$

Buffer which may be regarded as being "good" buffer must fulfill the following conditions :

1) Must not bind with the metal ion.

2) The concentration of buffer must be sufficiently high to ensure that the hydrogen ion concentration remain constant (normal buffering).

3) The proton-transfer step must be faster than the metallation step. Then, the observed rates will be independent of the buffer (kinetic buffering).

However, if an insufficient concentration of buffer is used, the observed rate will be a function of buffer concentration.

1.6) Statistical Factor for Id Mechanism

Eigen[18,19] has proposed the observed formation rate constant for the interchange dissociative mechanism to be $K_{os}k_1$.

There are conflicting interpretation in the literature on whether $k_1 = k_{ex}$ or $k_1 = S'k_{ex}$ where S' is a statistical factor, and k_{ex} is the first-order rate constant for exchange of a particular solvent molecule from the first coordination sphere of the metal into the bulk solvent. This rate can be independently evaluated from O^{17}-NMR line width broadenings[20,21].

Suppose the outer-sphere coordination number is S, and that only one of the S sites is occupied by incoming ligand molecule ,L, then the change that the incoming ligand is in a favorable position for entering into the hole left by the departing inner-sphere solvent molecule is (1/S). Therefore the rate k_1 should be roughly equal to (1/S) x k_{ex}. For the metal-aquo cation, $M(H_2O)_6^{2+}$, there are 6 equivalent water molecules and therefore the first-order complex formation rate constant k_1 will be (6/S) x k_{ex}[22].

Lin and Rorabacher[23], on the other hand, have ignored the statistical factor. They have instead attempted to calculate the actual magnitude of electrostatic interactions by considering steric and solvent effects, and proposed $k_f = K_{os}k_{ex}/P$ where P is introduced to account for apparent steric hindrance effects (including ligand conformational effects).

1.7) Hydrolysis of Ferric Ion Solution

The hydrolysis of inorganic Fe(III) solutions consists of several steps : (1) formation of low-molecular-weight species; (2) formation of a red cationic polymer ; (3) aging of the polymer,

with eventual conversion to oxide phases ; and (4) precipitation of oxide phases directly from low-molecular-weight precursors. The species that exist in aqueous Fe(III) solution[24-27] are Fe^{3+}, $FeOH^{2+}$, $Fe(OH)_2^+$ and some formation of polynuclear species, $Fe_2(OH)_2^{4+}$ or Fe_2O^{4+} :

$$Fe^{3+} + H_2O \rightleftharpoons FeOH^{2+} + H^+ \qquad K_{11} \qquad (1.27)$$

$$Fe^{3+} + 2H_2O \rightleftharpoons Fe(OH)_2^+ + 2H^+ \qquad K_{12} \qquad (1.28)$$

$$2Fe^{3+} + 2H_2O \rightleftharpoons Fe_2(OH)_2^{4+} + 2H^+ \qquad K_{22} \qquad (1.29)$$

The values obtained by Hedström for equilibrium constants involved are the followings ;

K_{11} = 0.90×10^{-3}

K_{12} = 0.47×10^{-6}

K_{22} = 1.22×10^{-3} ($25^{\circ}c$, 3M $NaClO_4$ ionic medium)

Recently, Bino and Gibson[28,29] has proposed that hydrogen oxide bridging ligand ($H_3O_2^-$) may be an important intermediate in the hydrolytic process for mononuclear metal ion such as $Fe(H_2O)_6^{3+}$. Mössbauer spectroscopic study by Carrano and Spartalian[30] using Fe(EHGS) (EHGS: N-[2-(salicylideniimino)ethyl] (o-hydroxyphenyl)glycine.) shows that bridges of this type are expected to be pH dependent. At low pH, Fe(EHGS) is entirely in the aquo form ; at higher pH, near the pK_a, the aquo and hydroxo

forms coexist and may form hydrogen oxide brided dimers ; at pH higher than the pK_a, only the hydroxo form exists and the dimer disappears. This result supports the view of Bino and Gibson.

Thermodynamic data on Fe(III) hydrolysis have been reviewed or complied by Langmuir[24], Sylva[25], Baes and Mesmer[26], and Smith and Martell[27].

1.8) Aquo-Ligand Complexes of Iron(III) Metal Ion

Of all the first-three ions of the first transition metal series, Fe(III) has been one of the most difficult to study kinetically. This has been due to the fact that the free metal ion readily hydrolyzes[31,32], even in moderatly acid solutions, to $FeOH^{2+}$, which can dimerize[33]. In addition, the complexing ligand can react with either the free ion or the $FeOH^{2+}$ species, or both[34]. Complexation pathways involving the protonated and unprotonated ligand, have been found for both Fe^{3+} and $FeOH^{2+}$. In many of the kinetic studies, the data could be interpreted on the basis of two or more kinetically ambiguous mechanism, e.g., by pathways involving Fe^{3+} + L or $FeOH^{2+}$ + HL. In such instances, it was necessary to choose between possible alternatives by examining the "resonableness"[35] of the rate constants obtained. It should be noted that the observed rate constant for complex formation of these metals generally has the form

$$k_{obsd} = k_1 + k_2/[H^+]$$

where k_1 and k_2 refer to the rate constants for complex formation for $Fe(H_2O)_6^{3+}$ and $Fe(H_2O)_5OH^{2+}$ respectively.

The rate constants given in table 1[36,37] are from studies in which the hydrogen ion concentration is varied.

Table 1 Summary of rate constants ($M^{-1}s^{-1}$) for various Fe(III) pathways

Ligand	Fe^{3+} + L	$FeOH^{2+}$ + L
Cl^-	9.4	1.1×10^4
	19	1.2×10^4
Br^-	50	4.1×10^4
	20	2.6×10^4
F^-	4×10^3	-
HF	11	3.1×10^3
SCN^-	1.27×10^2	1.0×10^4
SO_4^{2-}	6.4×10^3	-
	1.0×10^3	3×10^5
	$(3.5-4.6) \times 10^3$	1.1×10^5
HSO_4^-	38	5×10^4
	-	3×10^4
	-	1.4×10^5
$H_2PO_2^-$	2.7×10^2	-
H_3PO_2	13	2.1×10^4
N_3^-	1.6×10^5	-
	1.4×10^5	-
	-	$3 \times 10^3 - 4 \times 10^4$

Table 1 (continued)

Ligand	$Fe^{3+} + L$	$FeOH^{2+} + L$
HN_3	4	6.8×10^3
	2.6	7.4×10^3
	-	6.1×10^3
CH_3COO^-	3.4×10^5	-
CH_3COOH	4.8	5.3×10^3
$Fe(CN)_6^{3+}$	1.75×10^3	-
$ClCH_2COO^-$	4.9×10^3	2.8×10^4
$ClCH_2COOH$	2.2	6.8×10^3
$CH_3CH_2COO^-$	4.2×10^5	-
CH_3CH_2COOH	5.7	5.1×10^3
CrO_4^{2-}	5×10^7	-
$HCrO_4^-$	-	9.2×10^3
$HC_2O_4^-$	11.4×10^2	-
	8.6×10^2	-
C_6H_5OH	25	7.2×10^2
$C_6H_5O^-$	a	-
$C_6H_4(NH_2)OH$	-	1.1×10^5
$C_6H_4(NH_2)O^-$	a	-
$SSal^{3-}$	a	-
$SSalH^{2-}$	1.8×10^3	1.2×10^4
Sal^{2-}	a	-
$SalH^-$	-	1.4×10^4

** a values, if computed, would exceed the diffusion-controlled limit

1.9) The Scope of This Thesis

There are two main aspects of this research. One is the synthesis, and subsequent determination of pK_a of pyridoxal salicyloyl hydrazone. The second is to measure the rates of complexation between Fe(III) with pyridoxal benzoyl hydrazone and pyridoxal salicyloyl hydrazone and to deduce the reaction mechanism.

CHAPTER TWO

EXPERIMENTAL SECTION

In this chapter, appararus and general method used in the synthesis, the determination of pK_a and the kinetic experiments are presented. The experimental procedure and the method to determine the observed rate constants are also discussed.

2.1) Abbreviations and Symbols

The following lists are the common abbreviations, structural formulae and symbols used in this thesis

Abbreviation	Compound	Structure
PIH	pyridoxal isonicotinoyl hydrazone	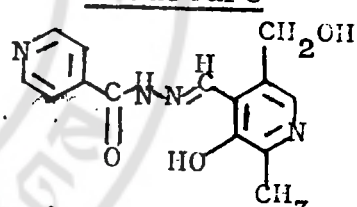
PBH	pyridoxal benzoyl hydrazone	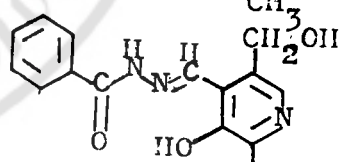
PSH	pyridoxal salicyloyl hydrazone	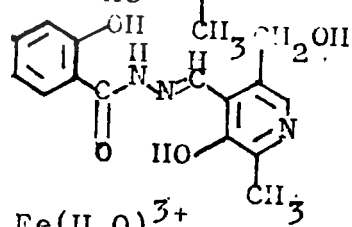
Fe^{3+}	hexaaquoiron (III) ion	$Fe(H_2O)_6^{3+}$
$FeOH^{2+}$	monohydroxoiron (III) ion	$Fe(H_2O)_5(OH)^{2+}$
$Fe(OH)_2^+$	dihydroxoiron (III) ion	$Fe(H_2O)_4(OH)_2^+$
$Fe_2(OH)_2^{4+}$	dimer of $FeOH^{2+}$	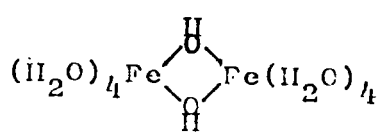

Abbreviation	Compound	Structure
Fe_2O^{4+}	dimer of $FeOH^{2+}$	$(H_2O)_4Fe—O—Fe(H_2O)_4$

Symbol	Name
A_∞	absorbance at infinite time
A_t	absorbance at time t
A_o	absorbance at initial time
I	ionic strength in mole litre^{-1}
K	equilibrium constant
k	rate constant
s	second
t	time
λ	wavelength in nanometer (nm)
[x]	concentration of x species in M
$[\bar{x}]$	concentration of x species in M at equilibrium
H_3L	fully-protonated PBH and PSH
H_2L^o	electrically neutral PBH and PSH
HL^-	mono-protonated PBH and PSH
L^{2-}	fully-dissociated PBH and PSH

2.2) Chemicals

The chemical used in this research and their grades are listed below

Chemical	Supplier	Grade
chloroacetic acid	BDH	AR
formic acid	May & Baker	AR
acetic acid	J.T.Baker	AR
potassium hydrogen phosphate	E.Merck	AR
disodium hydrogen phosphate	Fisher Scientific	AR
trishydroxylamine hydrochloride	SBR	Pro-analysi
sodium tetraborate decahydrate	J.T.Baker	AR
boric acid	J.T.Baker	AR
potassium hydroxide	BDH	AR
sodium chloride	E.Merck	Pro-analysi
hydrochloric acid	E.Merck	Pro-analysi
nitric acid	J.T.Baker	AR
methyl red	E.Merck	Indicator
ammonium hydroxide	E.Merck	AR
sodium nitrate	E.Merck	AR
tritiplex (EDTA)	E.Merck	AR
iron(III) nitrate nonahydrate	E.Merck	Pro-analysi
pyridoxine hydrochloride	E.Merck	AR
salicyloyl hydrazide	SIGMA	AR
manganese oxide activated	Fluka	Akiviert

2.3) Spectrophotometers

1) UV-Visible Spectrophotometer

All the kinetic runs and pK_a measurements were carried out on the Beckman Acta V spectrophotometer. Spectra were recorded using the Jasco Graphicard spectrophotometer.

2) IR-Spectrophotometer

IR-spectra were recorded using the Jasco IR-spectro - photometer.

3) [illegible] - spectrophotometer

The concentration of Fe^{3+} ion was determined by the Instrumentation Laboratories AA-spectrophotometer.

2.4) Thermostatting

The temperature of UV-Visible spectrophotometer cell compartment and the solution for kinetic measurements, pK_a measurements and pH measurements was controlled by Colora Kryothermostat W 5, as the cooling system, with Colora NB 3DSE water bath, as the circulating system.

2.5) pH-Meter

The pH of solution was measured using the Beckman digital pH-meter Model 1350 with a Beckman glass electrode and Corning calomel reference electrode. The standard buffer used to calibrate the meter were acetic acid-sodium acetate (pH 4.00), standard phosphate (pH 7.00) and standard borate (pH 9.00). Calibration curve of pH against concentration of standard HNO_3

is shown in Fig 2.1.

Table 2.1 pH of various nitric acid solutions at I = 0.30 and T = 25°c

No.	$[H^+]$, mM	pH
1	18.0	1.79
2	22.5	1.61
3	25.2	1.56
4	30.0	1.49
5	36.0	1.41
6	45.0	1.31
7	54.0	1.23
8	64.8	1.15
9	72.0	1.10
10	86.4	1.03
11	90.0	1.00
12	111.7	0.93
13	134.0	0.85

2.6) Preparation and Chemical Analysis of Materials

2.6.1) Double-distilled Water

The laboratory distilled water was redistilled and the double-distilled water used to prepare solutions.

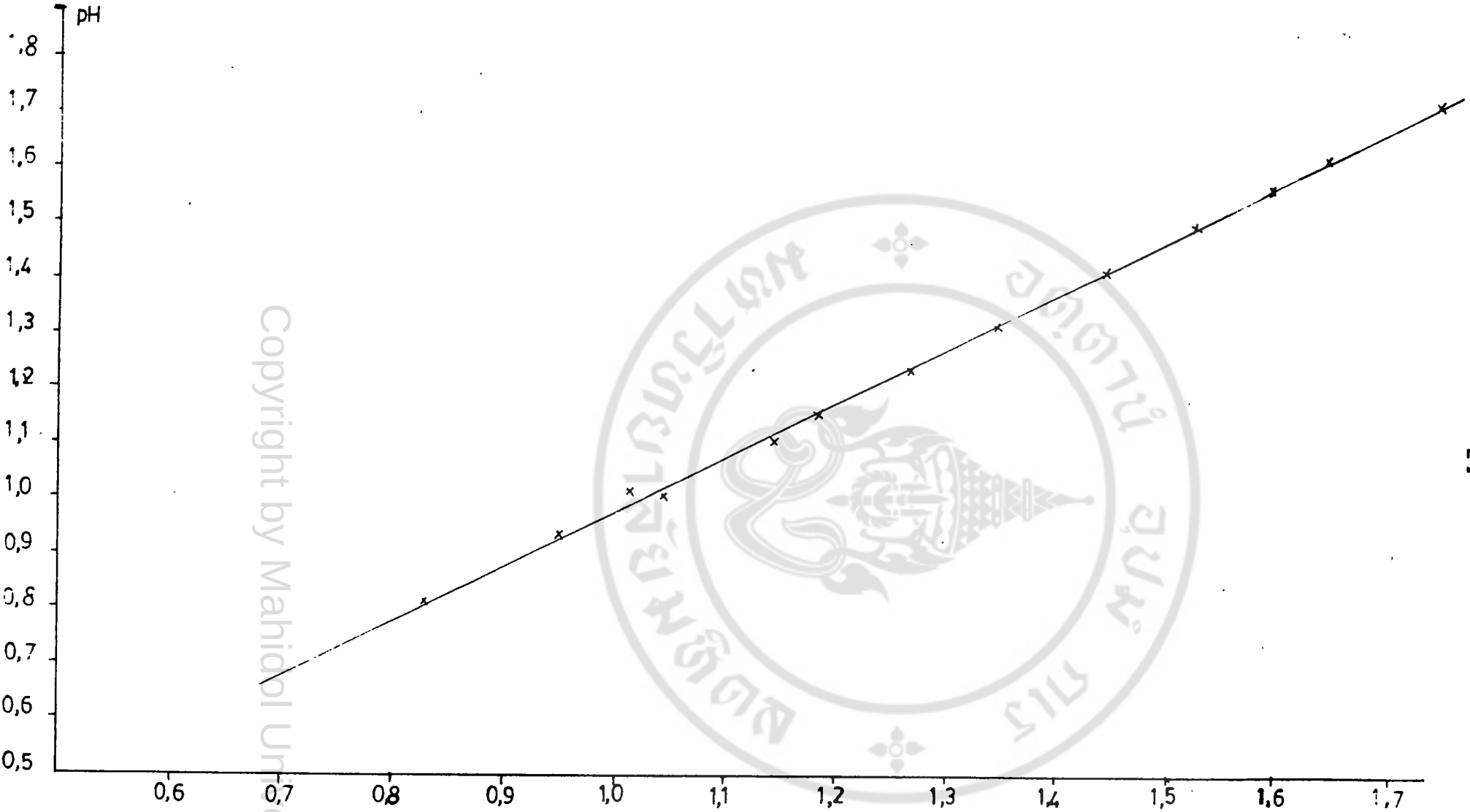

Fig 2,1 Calibration curve of observed pH aginst $[HNO_3]$ at $I = 0,3\ M\ (NaNO_3)$ and $T = 25^{\circ}C$

2.6.2) Nitric Acid Solution

Nitric acid solution are prepared from concentrated nitric acid. The concentration of the solution was determined by titrating with sodium borate solution using methyl red as indicator[38].

2.6.3) Ferric Nitrate Solution

The stock solution was prepared by dissolving $Fe(NO_3)_3 \cdot 9H_2O$ in a small amount of 1 N HNO_3. In order to prevent extensive hydrolysis, freshly prepared solution was used.

The concentration of Fe^{3+} ion was determined by Atomic Absorption Spectroscopy using standard ferric nitrate solution as the calibration curve.

Table 2.2 Calibration curve of standard ferric nitrate solution

Absorbance	$[Fe^{3+}]$, ppm
0.017	0.5
0.047	1.0
0.118	2.5
0.228	5.0

2.6.4) Pyridoxal Salicyloyl Hydrazone

Pyridoxal salicyloyl hydrazone was prepared[39] by dissolving 1 g. of pyridoxine-HCl in H_2O and then treated with 0.48 g. H_2SO_4 and 0.5 g. Mn_2O. The mixture was then heated at 60-70°c 2.5 hrs. until the Mn_2O was dissolved. Excess Mn_2O was

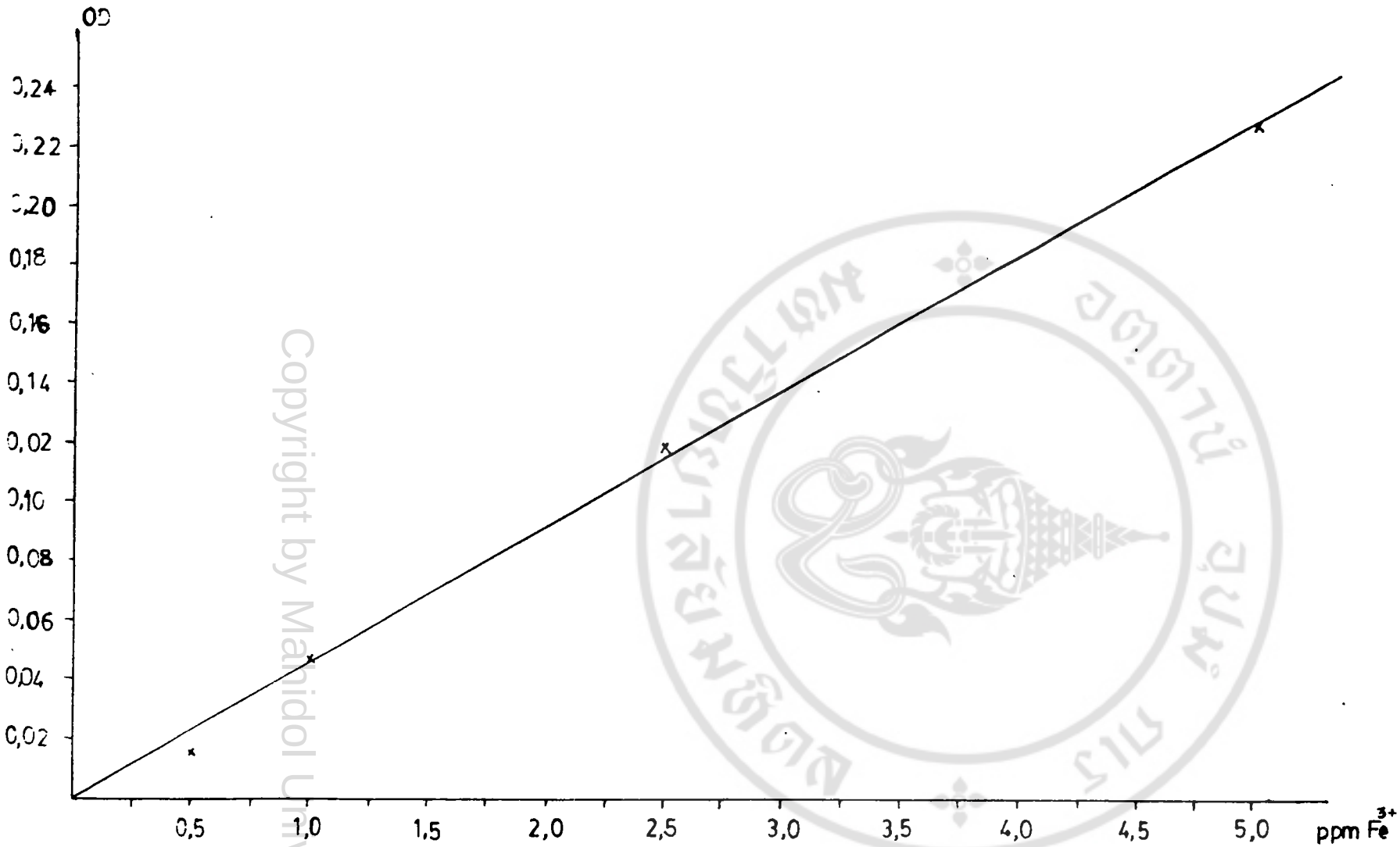

Fig 2,2 Calibration curve of standard ferric nitrate

filtered and the filtrate heated on an H_2O bath; 0.72 g. salicyloyl hydrazine in H_2O was then added, and the mixture filtered after 0.5 hr., yielding Mn-salt. EDTA in excess was dissolved in H_2O, made slightly basic with NH_4OH and added to the Mn-salt in H_2O to yield pyridoxal salicyloyl hydrazone. The crude product was recrystallized using hot MeOH to yield pale-yellow crystals, mp. 238-240°c (decomposition).

2.6.5) Pyridoxal Benzoyl Hydrazone

The compound was prepared by C. Sangma[40] using the same procedure as for PSH.

2.6.6) Pyridoxal Salicyloyl Hydrazone and Pyridoxal Benzoyl Hydrazone Solutions

The stock solutions were prepared by dissolving the reagents in water and heating to dissolve the particles, but never exceeding 70°c to avoid decomposition of the compounds. Working solutions of required concentration were prepared daily from the stock solutions. At the conditions used in the experiment, ligand hydrolysis was negligible.

2.7) General Experimental Procedure

2.7.1) pK_a Measurement of Pyridoxal Salicyloyl Hydrazone

Optical densities of PSH solutions were measured on a Beckman Acta V UV-Visible spectrophotometer, at

the fixed wavelength of 390 nm. Each solution contained PSII, buffer and NaCl (for adjusting the ionic strength to 0.10M) in a 25-ml volumetric flask. Series of buffer solutions with pH varying from 2.0 to 12.0 were prepared according to Perrin[41]. The solution was then kept at 25°c in water bath and the pH measured with the previously calibrated glass electrode. When the required pH was attained, 3 ml of solution was poured into the cuvette and kept in the cell compartment for further 2-3 minutes to equilibrate at 25°c. The absorbance was then read out and recorded.

2.7.2) Kinetic Measurements

The complex formation between $Fe(H_2O)_6^{3+}$ ion with PSII and PVI was studied on the Beckman Acta V spectrophotometer. Each solution was prepared in 25-ml volumetric flask. 1 M sodium nitrate solution was added to adjust the ionic strength of the solution to 0.30 M. The solution was then thermostatted at 25°c in the water bath and the pH of the solution was measured. The desired pH was obtained by adding 1 M HNO_3, never with NaOH, to avoid the formation of hydroxy species in solution. Then 1.5 ml of $Fe(H_2O)_6^{3+}$ solution was pipetted and transferred into a 1-cm path length cuvette which was placed a small magnetic stirrer at the bottom. As soon as the magnetic stirrer was turned on, 1.5 ml of ligand solution of equal pH value was transferred into the equilibrated metal solution. The reaction was thus initiated and the increase of absorbance due to the growth of the complex was

observed at the monitoring wavelength. The reaction was followed until the equilibrium state was established, i.e. until the absorbance was constant with respect to time.

2.8) Treatment of Data

2.8.1) For pK_a Measurements

The pK_a values of pyridoxal salicyloyl hydrazone were determined by equation

$$d = \frac{d_{HL}K_{a1}[H^+] + d_{H_2L}K_{a1}K_{a2}[H^+]^2 + d_{H_3L}K_{a1}K_{a2}K_{a3}[H^+]^3}{1 + K_{a1}[H^+] + K_{a1}K_{a2}[H^+]^2 + K_{a1}K_{a2}K_{a3}[H^+]^3}$$

by using non-linear least squares fitting programm to solve the solutions. The reported values are average of at least three experiments.

2.8.2) For Kinetic measurements

In order to simplify the rate expression and to ensure that the 1:1 complex was formed, all the reactions were run under pseudo-first order condition, i.e., the total concentration of Fe(III) ion must be much higher than the concentration of the ligand by at least a factor of 10. Thus the relation between absorbance and time is exponential.

The observed rate constant, k_{obsd}, were obtained from the slope of the plot of $\ln (A_\infty - A_t)/(A_\infty - A_o)$ vs time. The reported rate constants are average values of at least three kinetic runs.

CHAPTER THREE

RESULTS AND MECHANISM

3.1) Analytical Properties of Pyridoxal Salicyloyl Hydrazone

3.1.1) IR-Spectroscopy

The spectrum shows at least one strong absorption between 1650 and 1700 cm^{-1} which is due to C=O stretch. The C=N stretch occurs between 1600 and 1700 cm^{-1}. The compound under study is expected to display this absorption at the lower end of the range due to conjugation with an aromatic ring and the hydrogen bonding between the imino nitrogen and o-hydroxyl group. The skeletal ring vibrations occur in the same region, and hence the C=N stretch appears as a shoulder.

The 1700-1600 cm^{-1} region of the spectum for this compound is significant because both the C=O and C=N groups are involved in binding to the metal.

3.1.2) UV-Visible Spectroscopy

Like PLP in poly protic acid, its UV-vis spectrum change with pH. In acid solution, PSH absorb at 300 and 350 nm. As the pH is raised to 4, the absorption maxima at 390 and 410 nm develop whilst the other bands increase in intensity. An isosbestic point at 360 nm indicates an equilibrium between two species. This change is attributed to the deprotonation of the phenolic group of pyridoxal ring. From pH 7, 9 and 11, the 390 nm band increases and the one at 295 nm decreases, with an isosbestic point at 330 nm. These changes are attributed to pyridoxal ring N deprotonation.

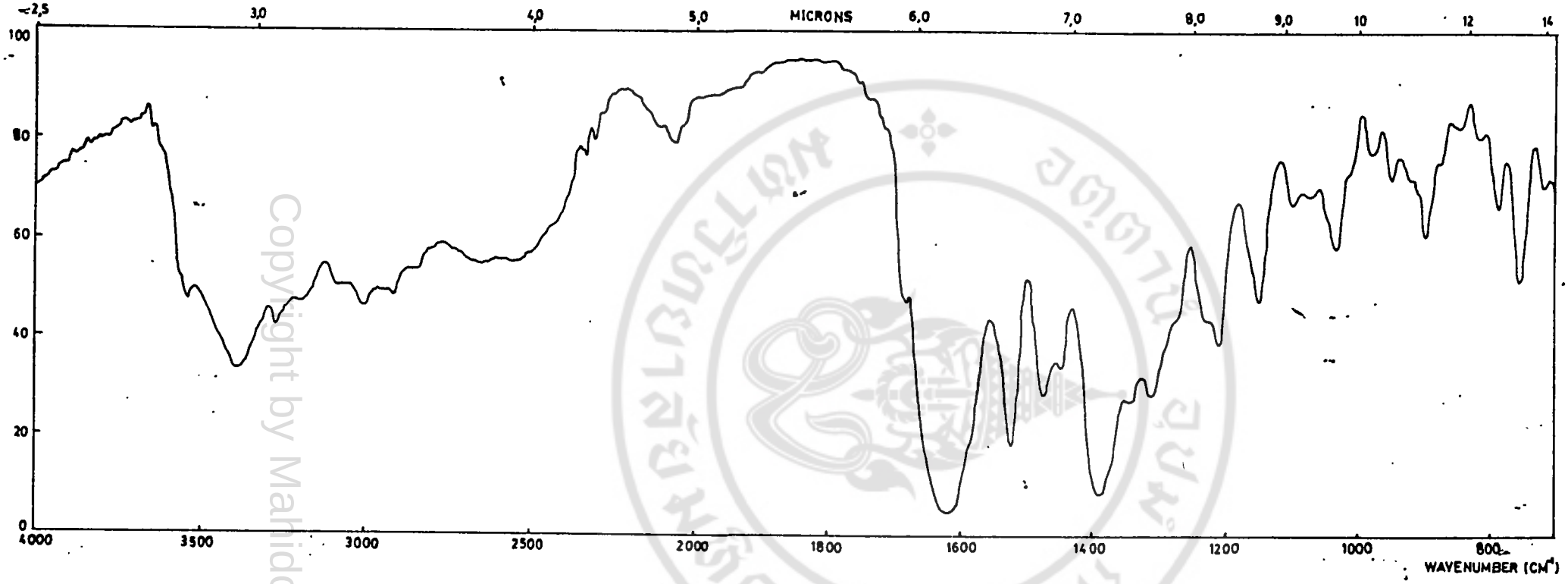

Fig 3,1 IR-spectra of PSH (sampling method ; KBR disc)

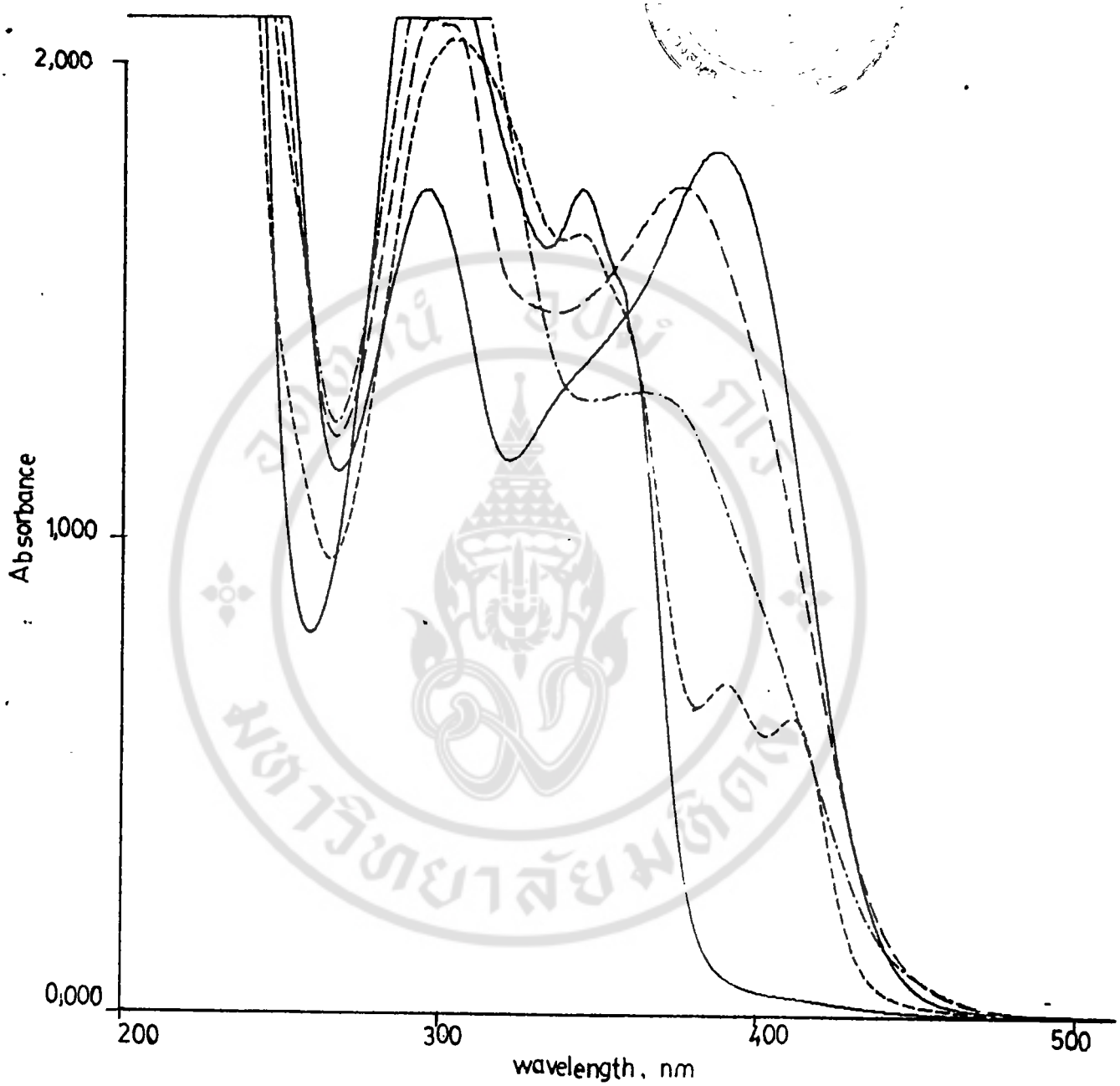

Fig 3,2 UV – Visible spectra of PSH at various pH,

pH = 2,19 (—) , pH = 4,05 (- - - - -)

pH = 6,88 (—·—·—), pH = 9,31 (— — — —)

pH = 12,0 (—)

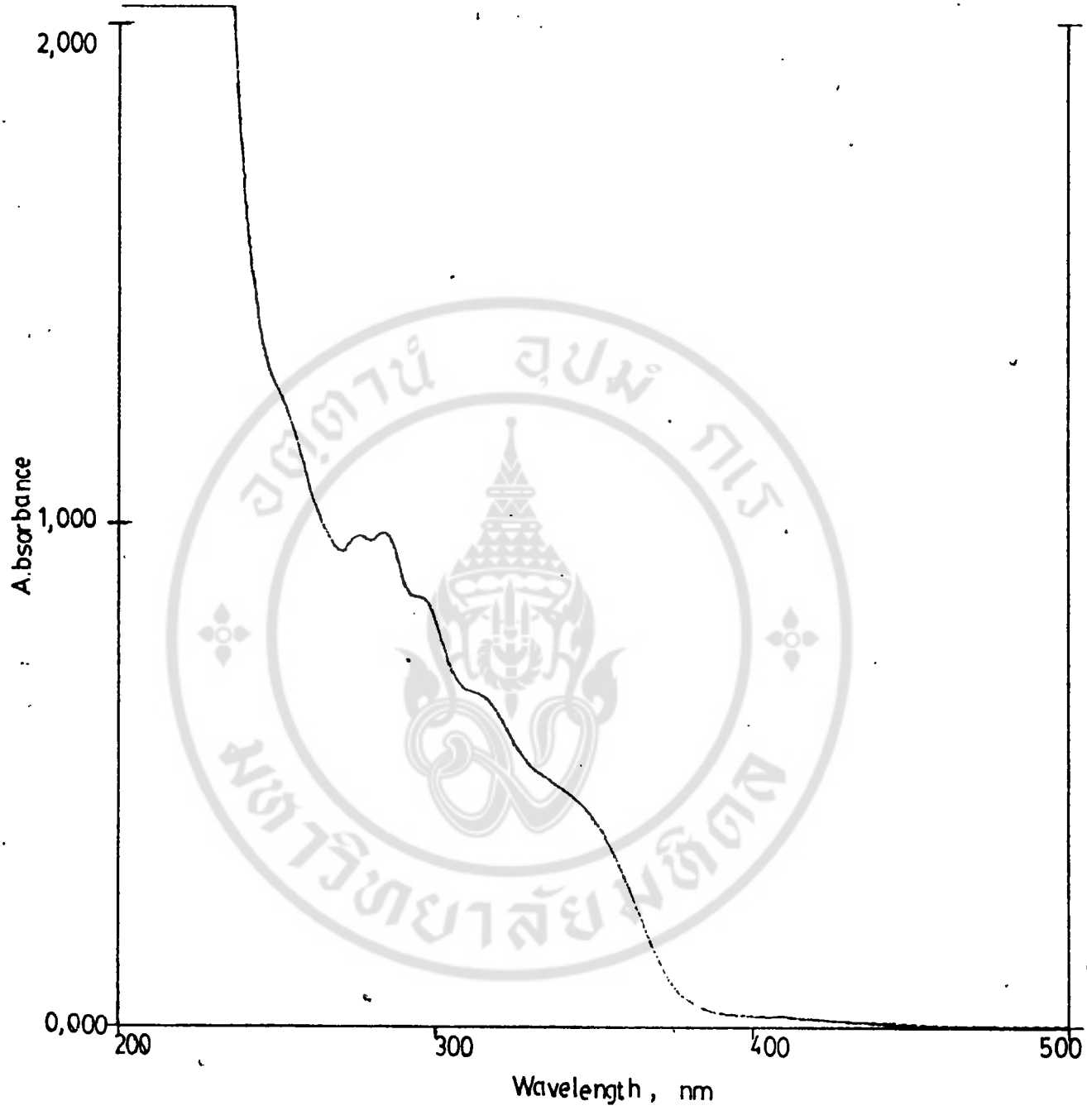

Fig 3,3 UV-visible spectra of free PSH in MeOH

3.2) pK_a Measurement

The experimental conditions for the measurement of acid association constants of pyridoxal salicyloyl hydrazone were :

$[PSH]$ = 1×10^{-3} M

pH = 2.0-12.0

I = 0.1 M (NaCl)

T = 25°c

Monitoring wavelength = 390 nm.

To calculate the acid association constants of PSH, the following mechanism is proposed (charges are omitted for simplicity and the solvated proton written as H^+),

$$L + H^+ \underset{}{\overset{K_{a1}}{\rightleftharpoons}} HL + H^+ \overset{K_{a2}}{\rightleftharpoons} H_2L + H^+ \overset{K_{a3}}{\rightleftharpoons} H_3L \qquad (3.1)$$

The various association constants are defined as follows,

$$K_{a1} = \frac{[HL]}{[L][H^+]} \qquad (3.2)$$

$$K_{a2} = \frac{[H_2L]}{[HL][H^+]} \qquad (3.3)$$

$$K_{a3} = \frac{[H_3L]}{[H_2L][H^+]} \qquad (3.4)$$

by using the relations,

$$\varepsilon_{H_3L}L_T = d_{H_3L} \quad (3.5)$$

$$\varepsilon_{H_2L}L_T = d_{H_2L} \quad (3.6)$$

$$\varepsilon_{HL}L_T = d_{HL} \quad (3.7)$$

$$\varepsilon_{L}L_T = d_{L} \quad (3.8)$$

and $$L_T = H_3L + H_2L + HL + L \quad (3.9)$$

leading to the equation,

$$d = \frac{d_L + d_{HL}K_{a1}[H^+] + d_{H_2L}K_{a1}K_{a2}[H^+]^2 + d_{H_3L}K_{a1}K_{a2}K_{a3}[H^+]^3}{1 + K_{a1}[H^+] + K_{a1}K_{a2}[H^+]^2 + K_{a1}K_{a2}K_{a3}[H^+]^3} \quad (3.10)$$

Non-linear least squares analysis was used to calculate pK_{a1}, pK_{a2} and pK_{a3}.

Where $$K_{a1} = 10^{-pK_{a1}} \quad (3.11)$$

$$K_{a2} = 10^{-pK_{a2}} \quad (3.12)$$

$$K_{a3} = 10^{-pK_{a3}} \quad (3.13)$$

$$[H^+] = 10^{-pH} \quad (3.14)$$

Thus, the averaged value for the association constants of pyridoxal salicyloyl hydrazone are,

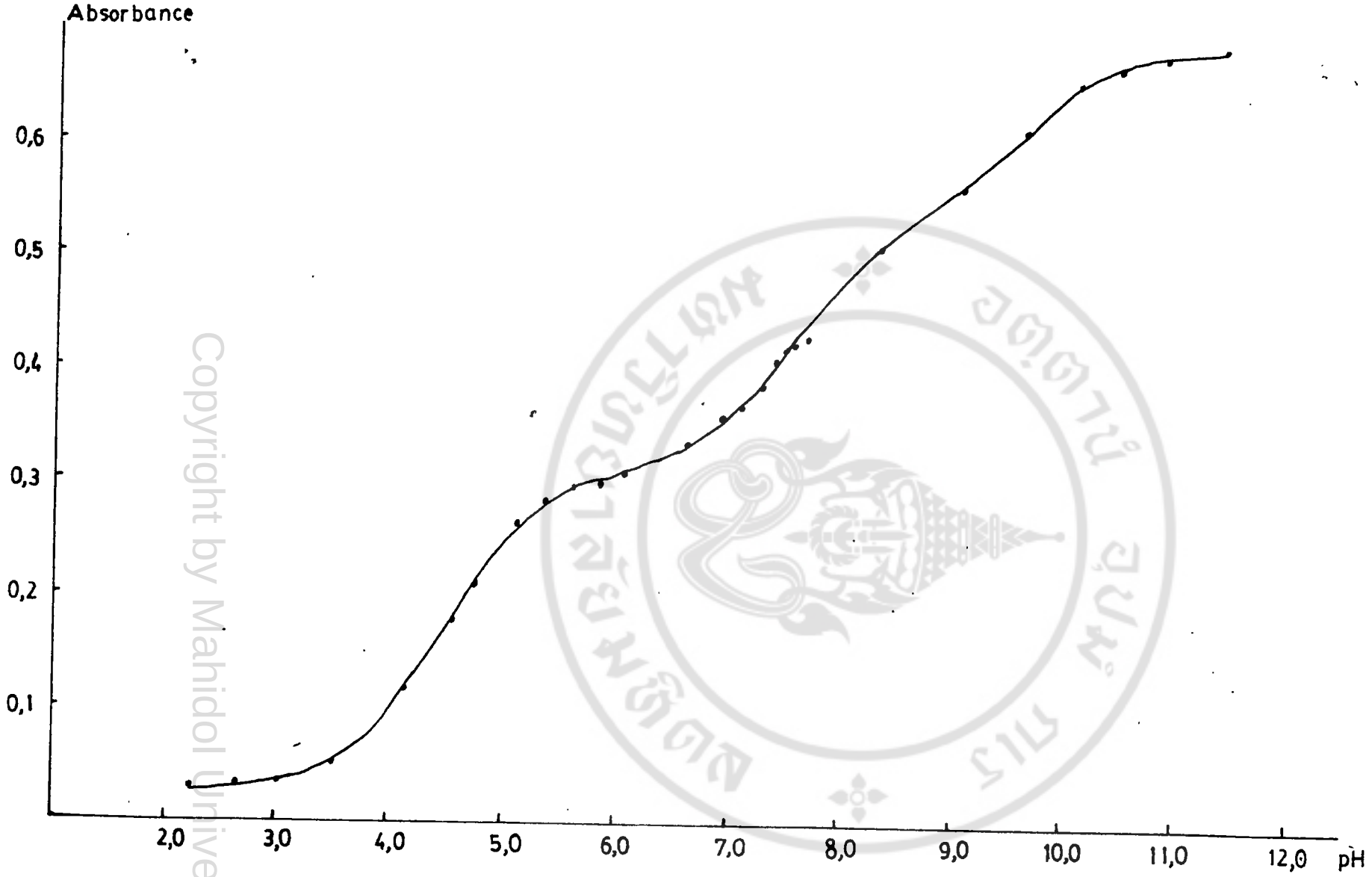

Fig 3,4 Absorbance of PSH at various pH, λ = 390 nm. conc. ca 1×10^{-3} M PSH, I ≤ 0,1M (NaCl) and T = 25 °C

pK_a	Assignment
4.48 ± 0.02	-OH (pyridoxal ring)
7.45 ± 0.13	ring N
9.42 ± 0.16	NH-N

3.3) Kinetic Measurements

3.3.1) Kinetic of Fe(III) Ion and Pyridoxal Benzoyl Hydrazone

The experimental conditions generally employed in this kinetic study were :

$[Fe(III)]_T$ = 3.8-11.5 x 10^{-3} M

[PBH] = ~4 x 10^{-4} M

$[H^+]$ = 0.02-0.2 M

I = 0.30 M ($NaNO_3$)

T = 25°c

Buffer = 0.02 M

monitoring wavelength = 470 nm

The kinetic results are shown in table 3.1

Table 3.1 Kinetic data for the Fe(III)-pyridoxal benzoyl hydrazone system at 25°c and I = 0.30 M

$[H^+]$, M	$10^3[Fe^{3+}]_T$, M	$10^3 k_{obsd}$, s^{-1}
0.05	3.82	12.14
	5.73	17.85

Table 3.1 (continued)

$[H^+]$, M	$10^3[Fe^{3+}]_T$, M	$10^3 k_{obsd}$, s^{-1}
0.05	7.65	22.33
	9.56	29.81
	11.47	34.74
0.09	3.82	7.97
	5.73	11.28
	7.65	14.26
	9.56	16.89
	11.47	19.91
0.13	3.82	6.82
	5.73	9.16
	7.65	11.80
	9.56	14.90
	11.47	16.60
0.17	3.82	6.50
	5.73	7.80
	7.65	9.50
	9.56	12.28
	11.47	14.26

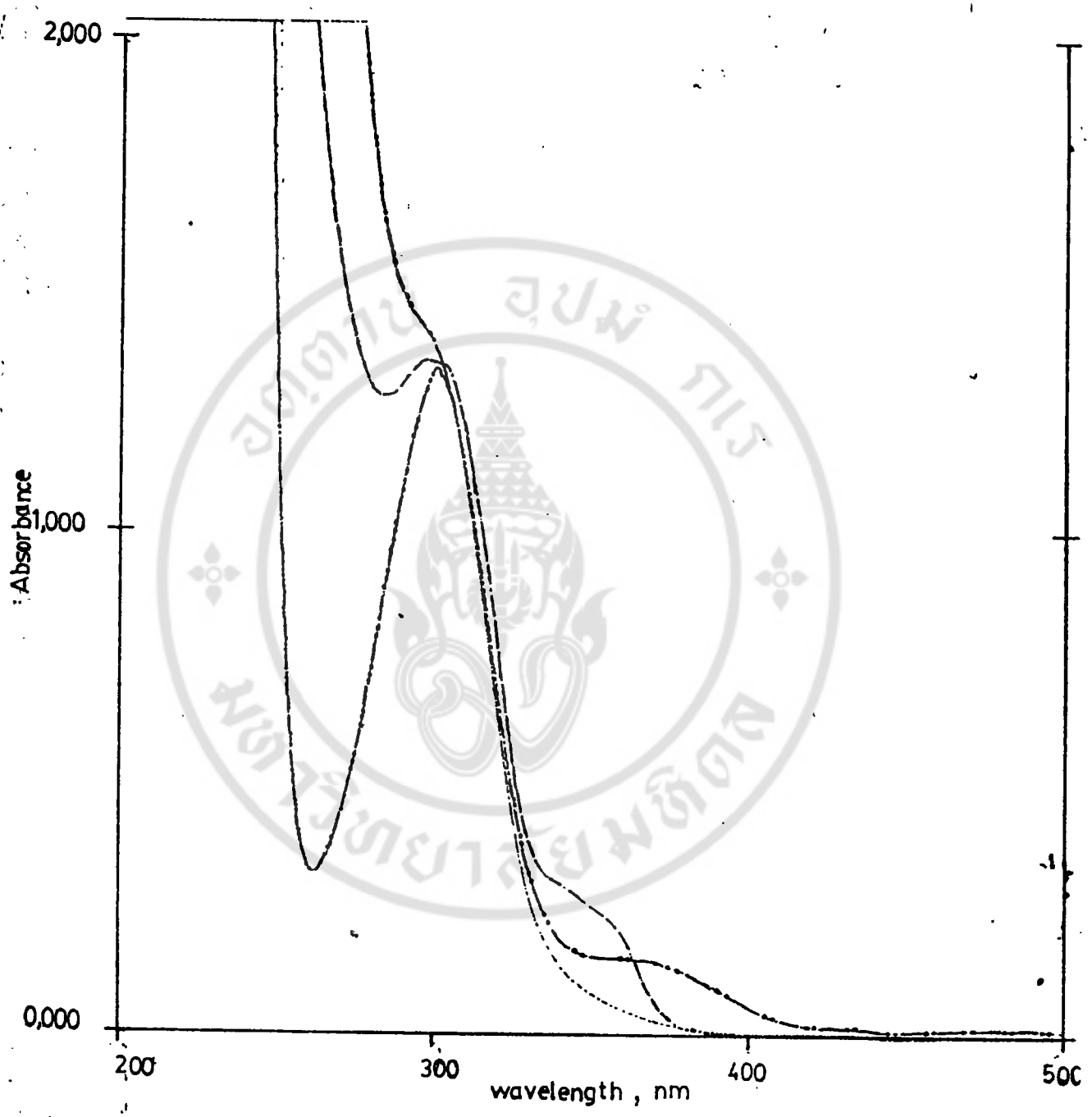

Fig 3,5 UV – Visible spectra of free PBH (——···——),
free Fe (III) (——·——) and Fe (III) – PBH complex (– – –)
at $[H^+]$ = 0,05 M conc.ca 8×10^{-5} M PBH, path length 1,0 cm

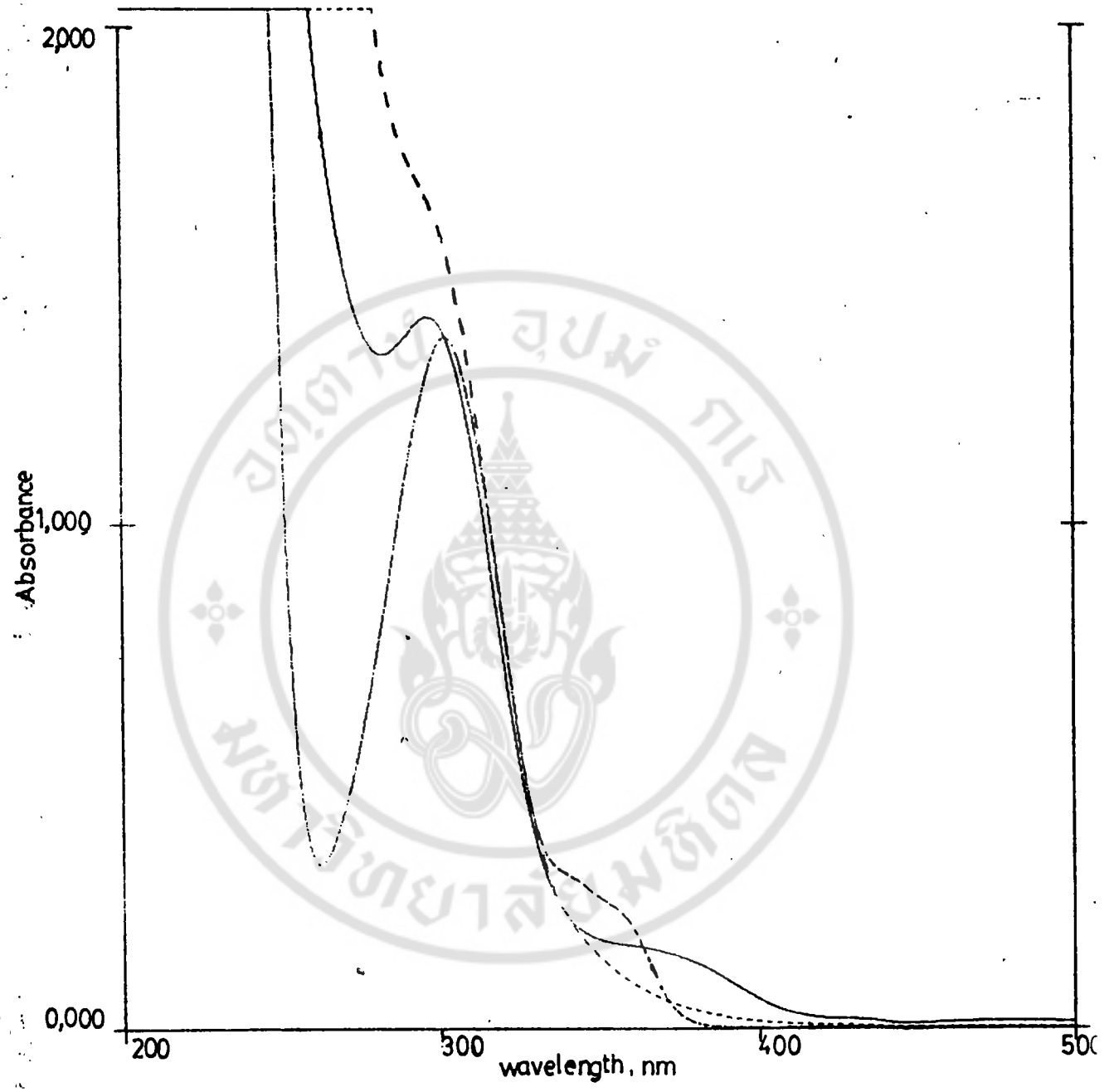

Fig 3,6 UV — Visible spectra of PBH (—·—), Fe(III) in chloroacetic acid buffer (---) and Fe(III) - PBH complex in chloroacetic buffer (—) at $[H^+]$ = 0,05M conc.ca 8×10^{-5} M PBH path length 1,0 cm.

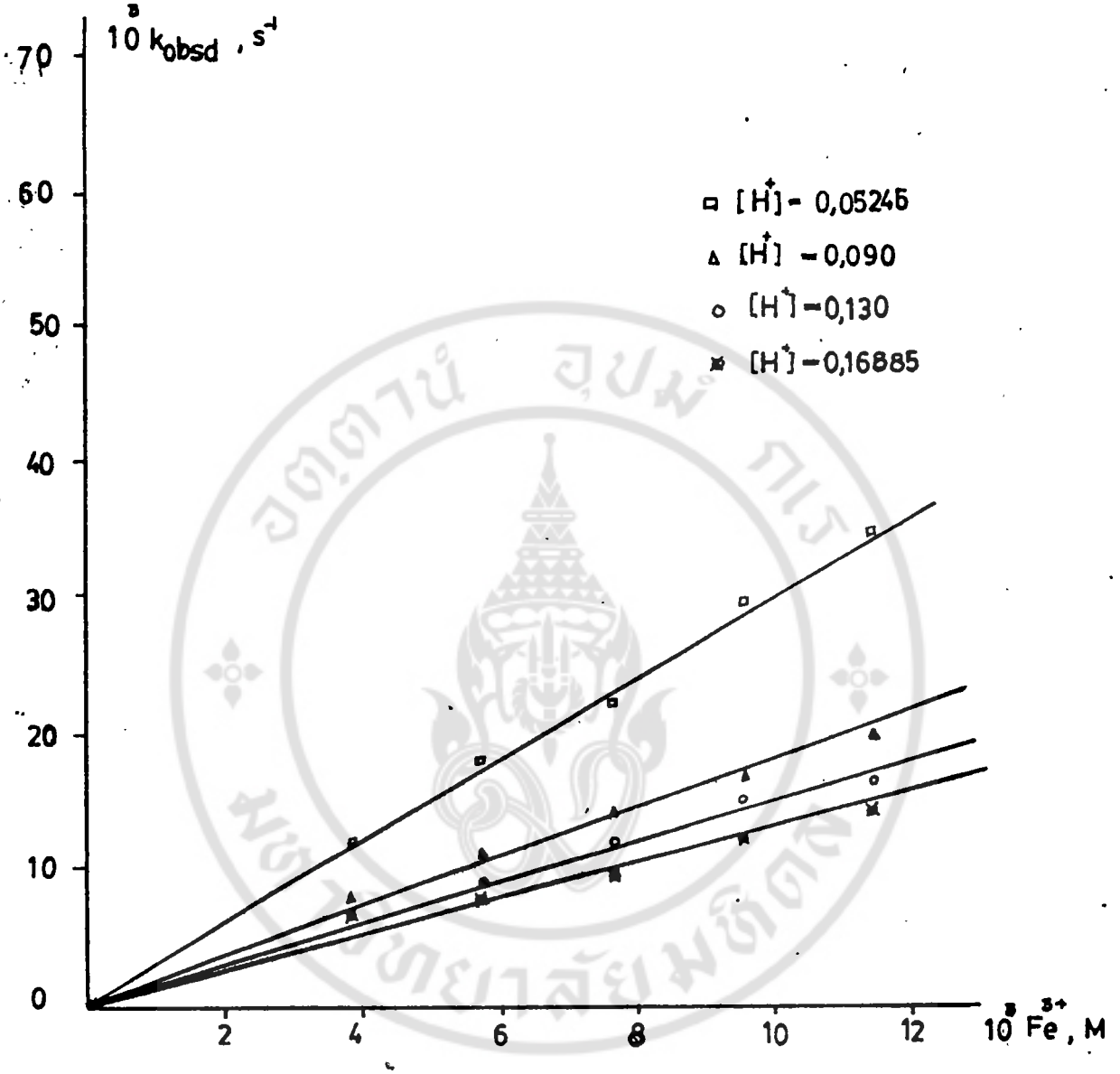

Fig 3,7 Value of k_{obsd} as a function of $[Fe^{3+}]_T$ for the reaction of Fe(III) - PBH at various $[H^+]$, I = 0,30 M ($NaNO_3$), T = 25°C

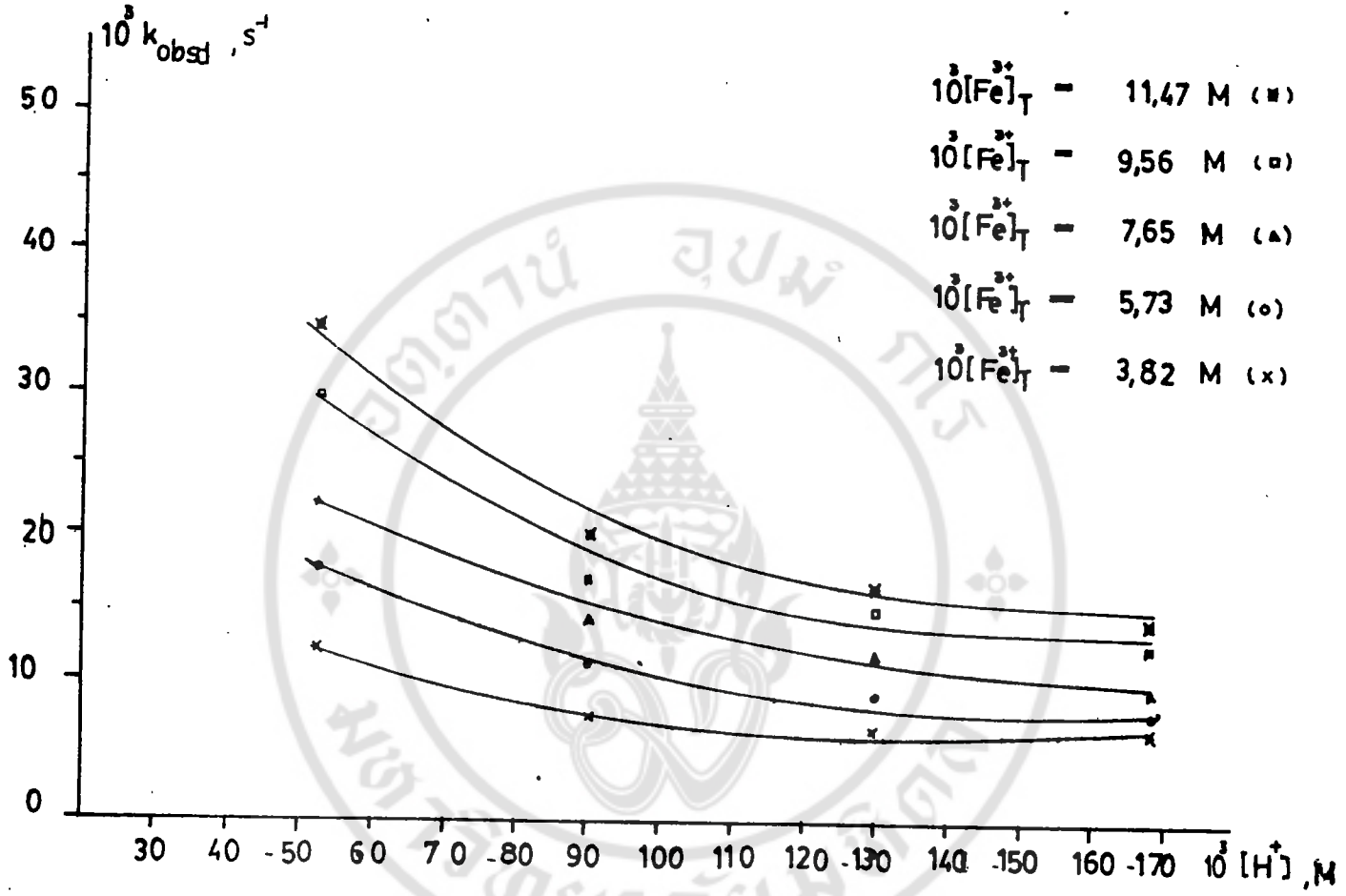

Fig 3,8 Value of k_{obsd} as function of $[H^+]$ for the reaction of Fe (III) – PBH at various $[Fe^{3+}]_T$, I = 0,30 M ($NaNO_3$), T = 25°C

3.3.2) Kinetic of Fe(III) Ion and Pyridoxal Salicyloyl Hydrazone

The experimental conditions generally employed in this kinetic study were :

$[Fe(III)]_T$ = 3.8-11.5 x 10^{-3} M

[PSH] = ~4 x 10^{-4} M

$[H^+]$ = 0.02-0.2 M

I = 0.30 M ($NaNO_3$)

T = 25°c

monitoring wavelength = 470 nm

The kinetic results are shown in table 3.2

Table 3.2 Kinetic data for the Fe(III)-pyridoxal salicyloyl hydrazone system at 25°c and I = 0.30 M

$[H^+]$, M	$10^3[Fe^{3+}]_T$, M	$10^3 k_{obsd}$, s^{-1}
0.05	3.82	12.29
	5.73	15.94
	7.65	20.05
	9.56	23.0
	11.46	26.37

Table 3.2 (continued)

$[H^+]$, M	$10^3[Fe^{3+}]_T$, M	$10^3 k_{obsd}$, s^{-1}
0.05	3.82	8.59
	5.73	10.75
	7.65	13.30
	9.56	15.02
	11.47	17.12
0.09	3.82	6.41
	5.73	8.12
	7.65	8.95
	9.56	12.16
	11.47	11.58
0.13	3.82	6.07
	5.73	6.78
	7.65	10.08
	9.56	11.48
	11.47	12.77

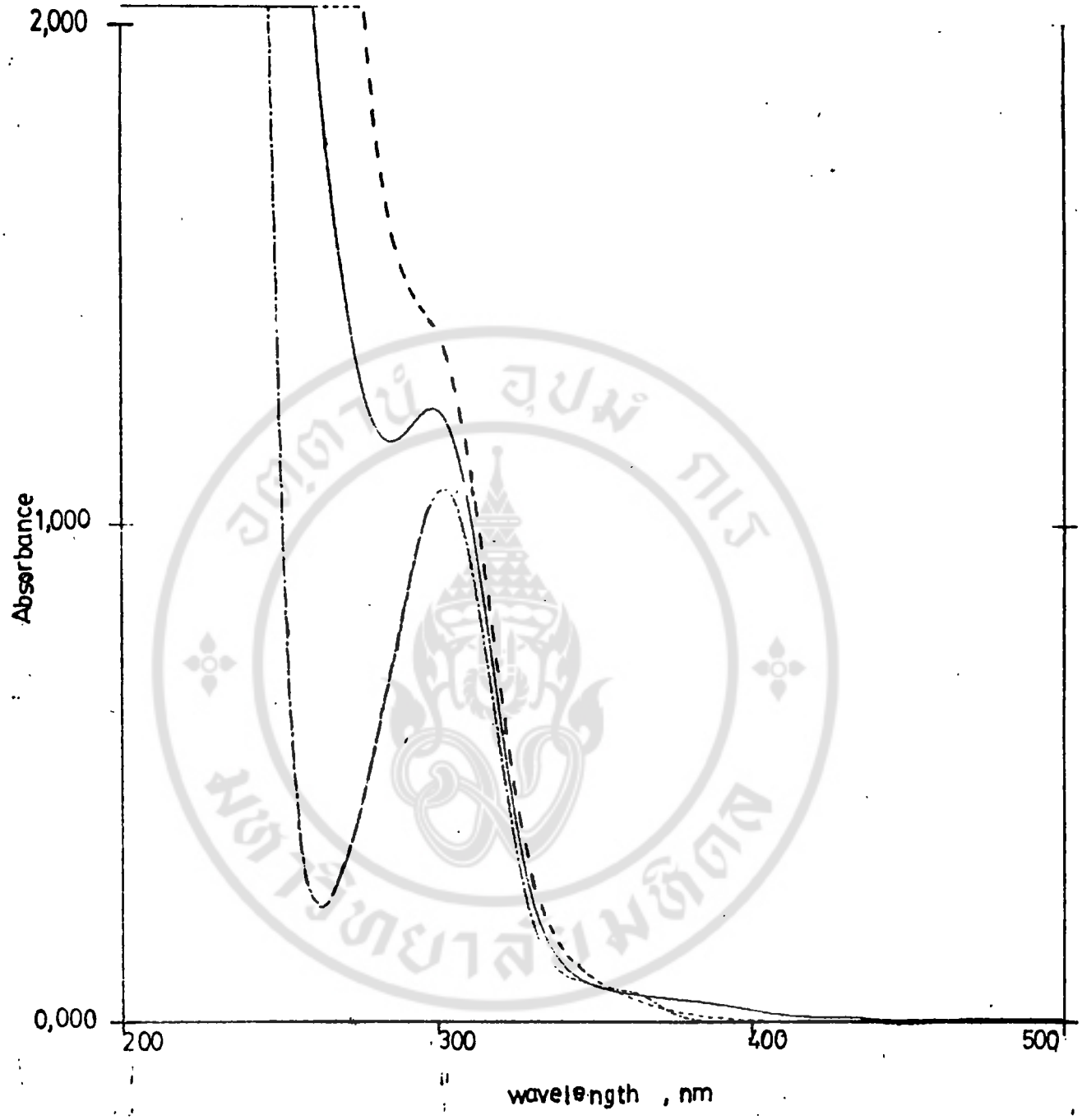

Fig 3,9 UV – visible spectra of free PSH (—···—) , free Fe (III) (- - -) and Fe (III) – PSH complex (——) at $[H^+]$ 0,05 M conc. ca 8×10^{-5} M PSH, path length 1,0 cm.

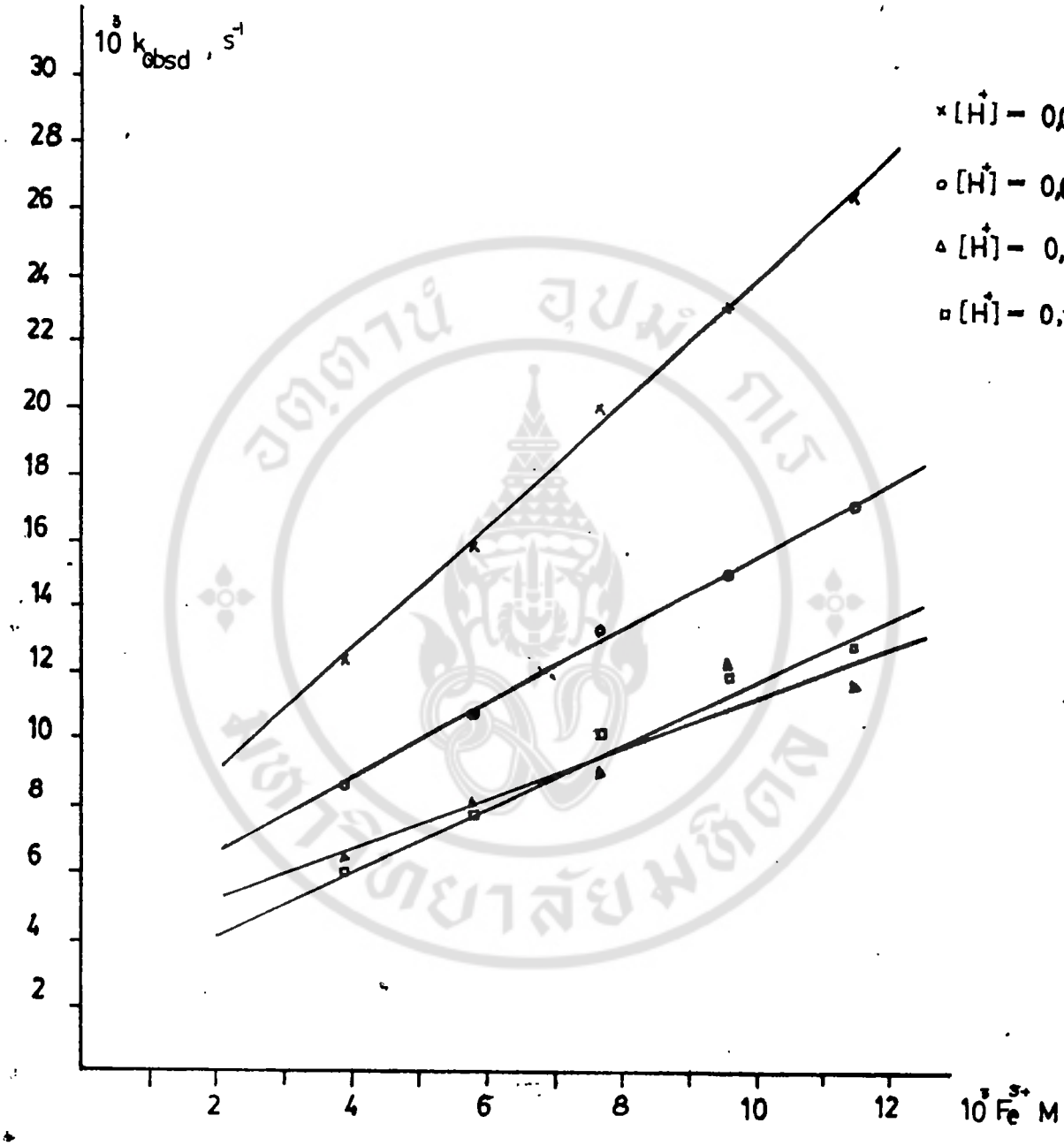

Fig 3,10 Value of k_{obsd} as a function of $[Fe^{3+}]_T$ for the reaction of Fe(III)– PSH at virious $[H^+]$, I = 0,30 M ($NaNO_3$), T = 25°C

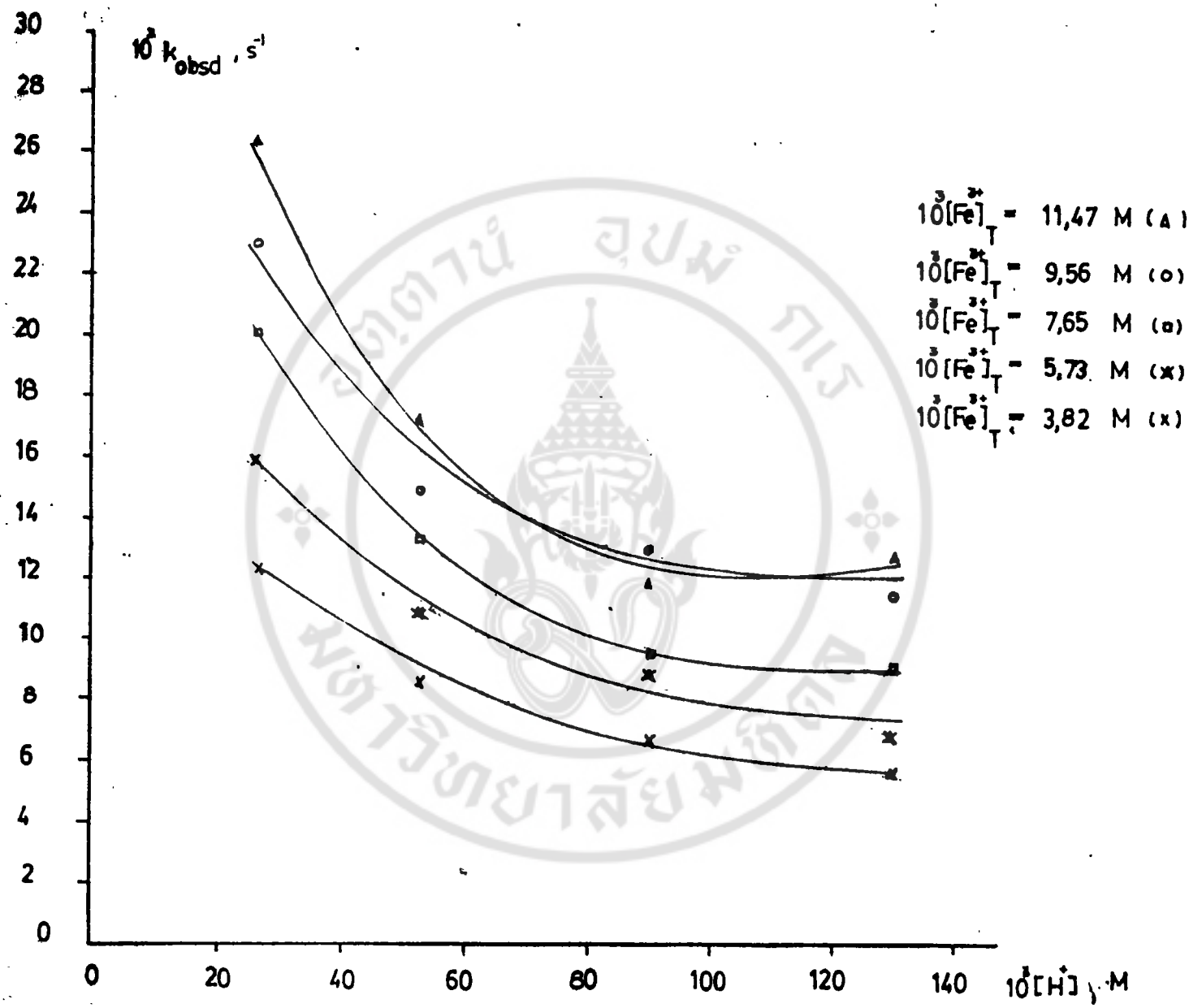

Fig 3,11 Valves of k_{obsd} as a function of $[H^+]$ for the reaction of Fe(III) - PSH at various $[Fe^{3+}]_T$ (I = 0,30 M ($NaNO_3$), T = 25°C)

From the kinetic data, the Fe(III)-PBH and Fe(III)-PSH system have the same characteristics which can be described as follows :

1) The measured rate constant, k_{obsd}, is a linear function of the total metal concentration, $[M]_T$, at a fixed pH, as shown in Figs. 3.7 and 3.10

2) At a fixed total metal concentration, $[M]_T$, the observed rate constant, k_{obsd}, decreases with increasing hydrogen ion concentration and reaches an asymptotic value at high concentration of hydrogen ion. (see Figs 3.8 and 3.11)

For the Fe(III)-PBH system chloroacetic acid was used. Its effect to the system was checked, the rate values were found to be independent of the buffering conditions.

3.4) Reaction Mechanism

Pyridoxal benzoyl hydrazone and Pyridoxal salicyloyl hydrazone have the structures (I) and (II) respectively

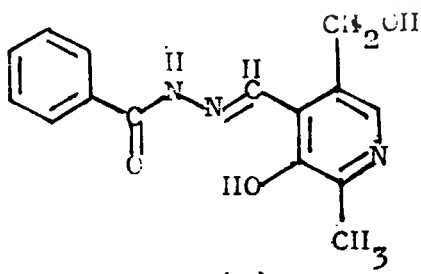

(I)

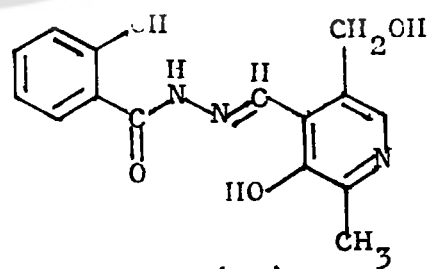

(II)

In this kinetic study, the concentration of nitric acid was sufficiently high to ensure that the hydrogen ion concentration remained constant during the kinetic run. The proton transfer step between ligand and solvent can be considered

to be much faster than the metallation step.

From the results of the kinetic study of complex formation between Fe(III) and the two hydrazones (PBH and PSH), and from the results of the potentiometric study by L. Vitolo[42] ($Fe(HL)^{2+}$ is the predominant species at pH not greater than 3.00 for the Fe(III)-PBH system and the species distribution as a function of pH for pyridoxal benzoyl hydrazone are H_3L^+ (pH 0-7), H_2L^o (pH 2-11), HL^- (pH 7-11) and L^{2-} (> 8)), then the following mechanism is proposed :

$$Fe^{3+} + H_3L^+ \underset{k_{-1}}{\overset{k_1}{\rightleftharpoons}} Fe(HL)^{2+} + 2\,H^+ \qquad (3.15)$$

$$\Big\uparrow\downarrow K_{OH}$$

$$FeOH^{2+} + H_3L^+ \underset{k_{-2}}{\overset{k_2}{\rightleftharpoons}} Fe(HL)^{2+} + H_2O + H^+ \qquad (3.16)$$

The equilibrium constant is defined as follows :

$$K_{OH} = \frac{[FeOH^{2+}][H^+]}{[Fe^{3+}]} \qquad (3.17)$$

The following assumptions must be applied :

1) The anion concentration of hydrazone, HL^-, L^{2-} and the electrically neutral species, H_2L^o is negligibly small as the medium is highly acidic and the pK_a of ligand is high.

2) The hydrogen ion concentration is sufficiently large so that $[H^+]$ may be regarded as constant during the kinetics.

The rate expression for this mechanism can be derived as follows :

$$-\frac{d[Fe(HL)^{2+}]}{dt} = -k_1[Fe^{3+}][H_3L^+] + k_{-1}[Fe(HL)^{2+}][H^+]^2 - k_2[FeOH^{2+}][H_3L^+] + k_{-2}[Fe(HL)^{2+}][H^+] \quad (3.18)$$

Mass balance equation :

$$\Delta[H_3L^+] = -\Delta[Fe(HL)^{2+}] \quad (3.19)$$

Pseudo-first order condition :

$$[Fe^{3+}] >> [H_3L^+] \quad , \quad [Fe^{3+}] = [Fe^{3+}]_T$$

Substituting in equation (3.4), we obtained the pseudo-first order rate constant

$$k_{obsd} = k_{-2}[H^+] + k_{-1}[H^+]^2 + \left[k_1 + k_2 K_{OH}/[H^+]\right][Fe^{3+}] \quad (3.20)$$

From the rate expression above, it can be clearly seen that

1) The observed rate constant, k_{obsd}, is a linear function of total metal concentration, $[M]_T$, at a constant pH (hydrogen ion concentration).

2) The dependency of the observed rate on hydrogen ion concentration, $[H^+]$, is a complicated non-linear function of hydrogen ion concentration as found experimentally. (see Figs. 3.8 and 3.11)

Equation (3.20) can be written as

$$k_{obsd} = a + b[M]_T \quad (3.21)$$

where

$$a = k_{-2}[H^+] + k_{-1}[H^+]^2 \quad (3.22)$$

$$b = k_1 + k_2 K_{OH}/[H^+] \quad (3.23)$$

The value of "b" from kinetic results are shown in table 3.3 and 3.4 for Fe(III)-PBH and Fe(III)-PBH systems respectively.

In order to evaluate k_1 and k_2, the values of "b" for various pH must be considered. If "b" is plotted against the reciprocal of hydrogen ion concentration, then the value of the slope and intercept would be ($k_2 K_{OH}/[H^+]$) and k_1 respectively. These are shown in Figs.3.12 and 3.13.

Value of K_{OH} (2.199×10^{-3}) is calculated as shown in appendix I. The values of all calculated rate constants are summarized in table 3.7.

Table 3.3 Experimental values of "b" for Fe(III)-PBH system at I = 0.30 and T = 25°c

$[H^+]$, M	$[H^+]^{-1}$, M	"b", $M^{-1}s^{-1}$
0.05	19.05	2.94
0.09	11.11	1.80
0.13	7.69	1.48
0.17	5.92	1.32

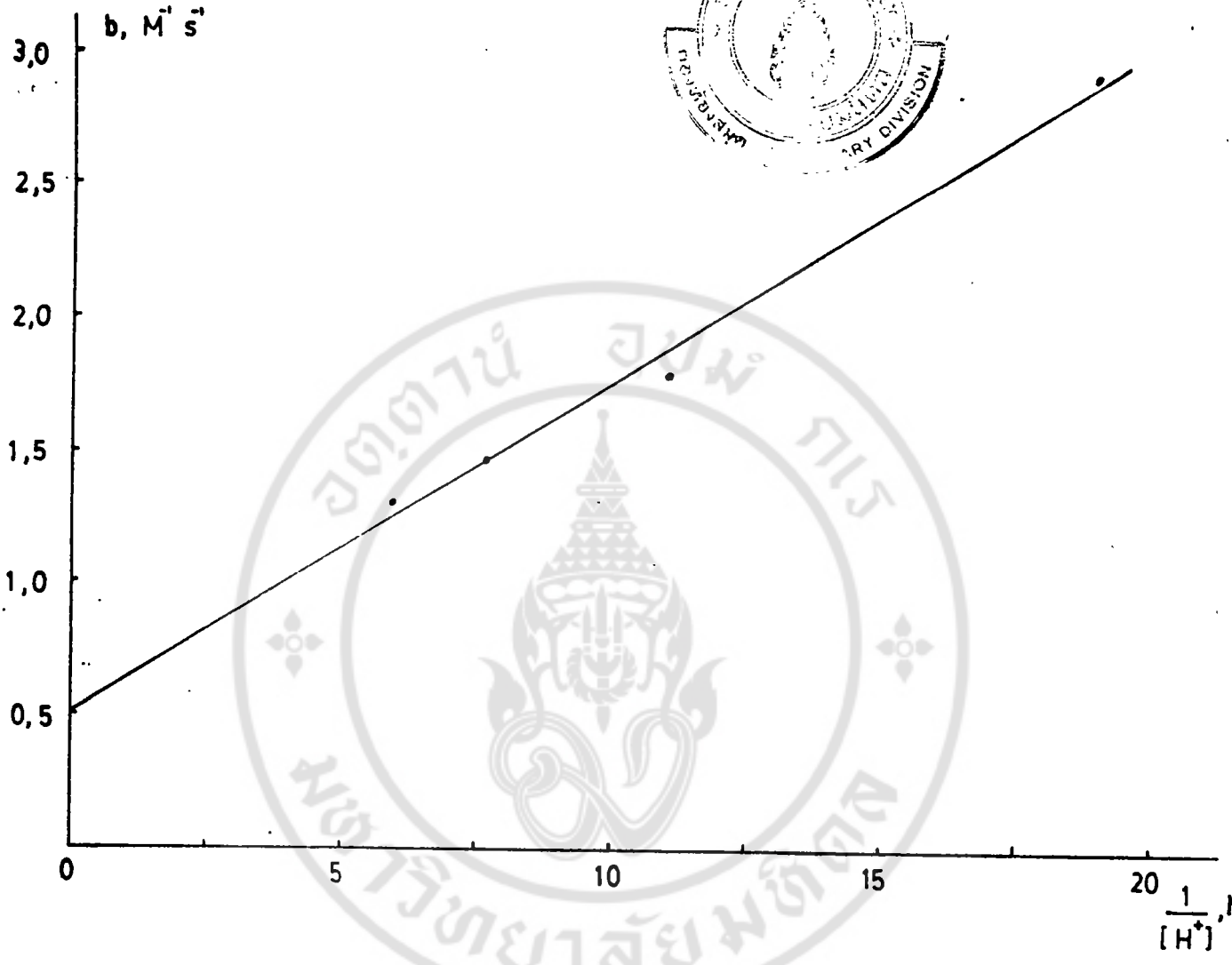

Fig 3,12 Dependence of b on $\frac{1}{[H^+]}$ for the reaction of Fe(III) - PBH at I = 0,30 M ($NaNO_3$) and T = 25°C

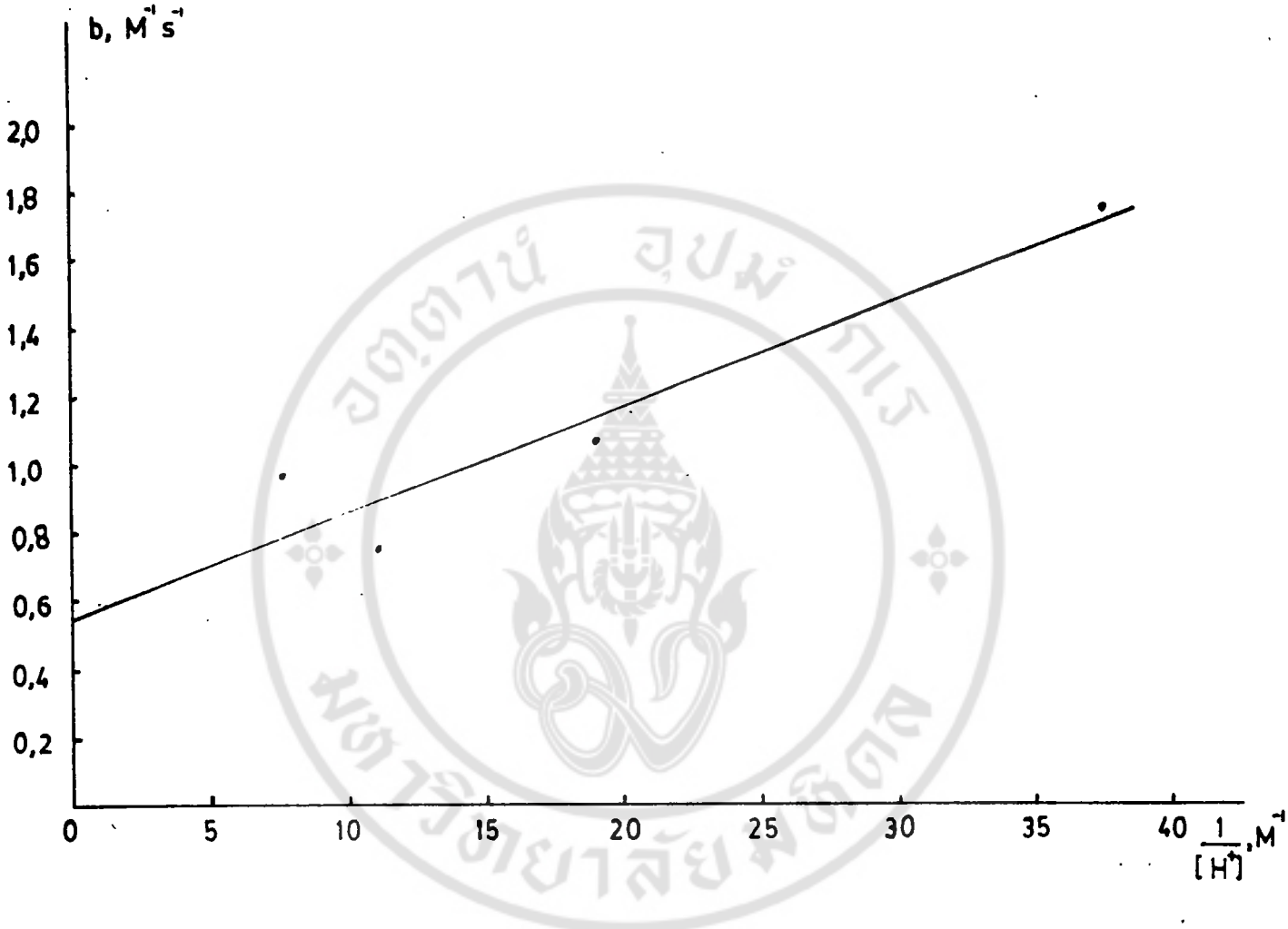

Fig 3,13 Dependence of b on $\frac{1}{[H^+]}$ for the reaction of Fe(III)-PSH at I = 0,30 M ($NaNO_3$) and T = 25 °C

Table 3.4 Experimental values of "b" for Fe(III)-PSH system at I = 0.30 and T = 25°c

$[H^+]$, M	$[H^+]^{-1}$, M	"b", $M^{-1}s^{-1}$
0.03	37.58	1.76
0.05	19.05	1.07
0.09	11.11	0.75
0.13	7.69	0.97

Table 3.5 Summary of rate constant for Fe(III)-PBH and Fe(III)-PSH system at I = 0.30 and T = 25°c

Rate Constant	Fe(III)-PBH	Fe(III)-PSH
k_1	0.52	0.55
$k_2 K_{OH}$	0.12	0.03
k_3	54.57	13.64

CHAPTER FOUR

DISCUSSION

L. Vitolo[42] has shown experimentally by potentiometric study that the species existing in solution in the pH range 2-14 for PBH are: H_3L^+, fully-protonated form; H_2L^o, electrically neutral species; HL^-, mono-protonated form and L^{2-}, fully-dissociated form. Thus for PSH, a ligand of nearly the same structure as PBH, these equilibria can be shown by scheme A ;

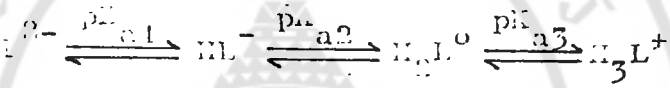

(I) (II) (III) (IV)

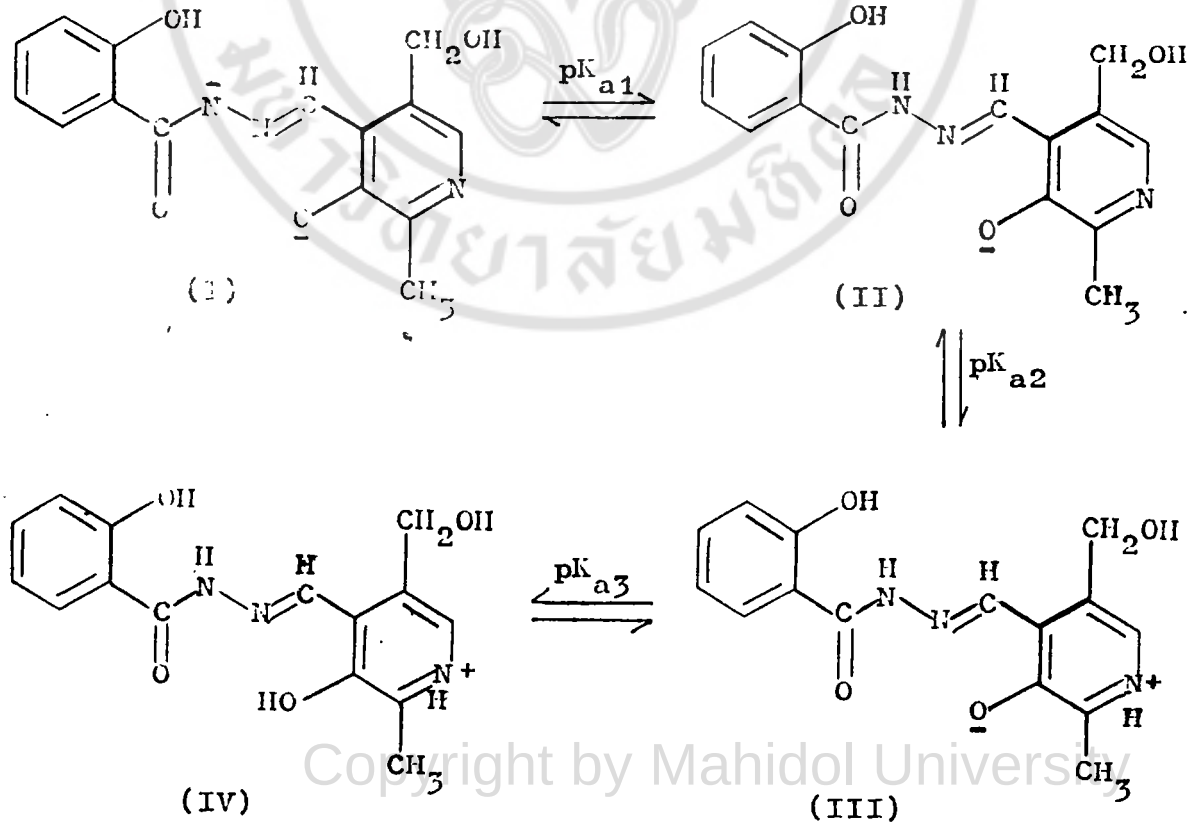

(I) (II) (IV) (III)

Scheme A

The existence of the electrically neutral species, H_2L^o at neutral pH suggests that PSH (also PBH) possess an important feature for an orally effective drug in that they may be able to pass through lipophilic membrane at physiological pH.

For the mechanism of the complex formation, a series of equilibria is proposed, which can be represented by scheme B.

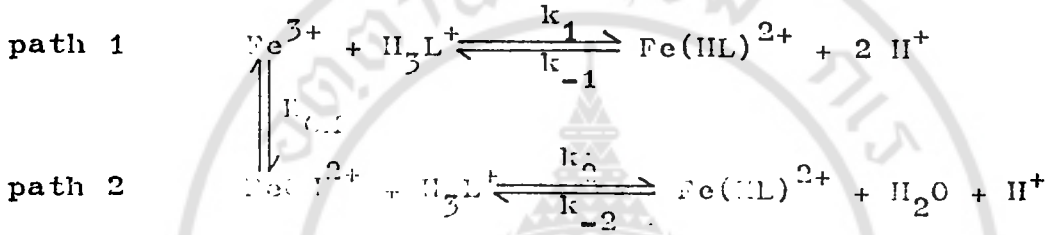

Scheme B

The reaction scheme above shows two parallel paths giving rise to the complex. The existence of the complex $Fe(HL)^{2+}$ has been shown by L. Vitolo in her potentiometric study. Anionic forms of the ligands, HL^-, L^{2-} and the electrically neutral species, H_2L^o are not considered for both ligands on the basis of their pK_a values[42]. The acidities used in this work were so high as to ensure that no anionic species exists in this condition. For the Fe(III)-PBH system, the buffering effect was checked and found that the observed rate constants of the system was independent on the buffering condition.

On considering the details of each reaction path and values of the rate constants for the forward reaction path (k_1 and k_2), it can be seen that k_1, k_2 are very much lower than that of literature values for various ligands reacting with $Fe(H_2O)_6^{3+}$ and

$Fe(H_2O)_5OH^{2+}$ [36,37,43]. Thus explanation must lie with factors causing a large decrease in the formation rate. Firstly there is the nonreactivity of the protonated ligand; the reaction path under study occurs via Fe^{3+} and H_3L^+, which has an unfavorable charge. For example J.C. Cassett and R.G. Wilkins[50] found that $^+NH_3CH_2CONHR$ is at least 10^3 fold less reactive than NH_2CH_2CONHR. T.J. Byadeley and K.H. Constant[51] measured the rate constants for the reaction of EDA^{2+} and $EDAH^-$ with Ni(II) which are 4.5×10^4 and 7.7×10^{-2} $M^{-1}s^{-1}$ at 25°c respectively, and NTA^{3-} and $NTAH^{2-}$, with rate constants 1.2×10^7 and 7.5 $M^{-1}s^{-1}$, showing 10^5 difference in reactivity[52]. Another example is the rate constants for reaction of enH^+ with Ni^{2+} which is about 10^2 less than that calculated for en (4×10^4 $M^{-1}s^{-1}$)[50], the difference residing in the unfavorable electrostatic effect for the protonated ligand. Secondly is the steric effect due to the difficulty of closing 6-membered ring as compared to 5-membered ring. Examples are the reaction between Co^{2+} and Ni^{2+} with α- and β-alanine[13], between α- and β-aminobutyrates with Ni^{2+} [14], between α- and β-diamines and histidine with Cu^{2+} [15]. From this, it may be concluded that one or all effects which causes a large decrease in the rate constants for the reaction between Fe^{3+} and PBH and PSH may be due to the difficulty of closing the 6-membered ring after 5-membered ring is formed. The very small rate constant probably arises from very unfavorable charge as well as steric hindrance considerations e.g. $terpyH_2^{2+}$ with Ni^{2+} (<0.5 $M^{-1}s^{-1}$)[54]. The terminal rings containing the protons are probably twisted slightly in opposite directions and

in this conformation the proton effectively block the lone pair electron of nitrogen. The last effect may be that of the intramolecular H-bonding of the ligands. For example three fold lower formation rate constant was observed for Hen^{+} relative to tmen^{+} [53] is explainable in the terms that a significant fraction of Hen^{+} species is intramolecularly H-bonded (in a "gauche in" conformational) and is thus unreactive toward the metal ion. Intramolecular H-bonding of PBH may occur between the imino nitrogen and the HO- of pyridoxal ring and sometimes the carbonyl oxygen, causing the most stable configurations (slowest rates). The more slower rates in PSH may be due to the third H-bonded between the amido nitrogen and the HO- of salicyloyl ring. Here a recombination with Fe^{3+} can occur only if the proton is liberated from the internal H-bond. Finally we can conclude that the substantially reduced rates for the reaction investigated here can be interpreted on the basis of ring-closure as the rate-determining step[15], as seen from both lower value for $Fe(H_2O)_6^{3+}$ and $Fe(H_2O)_5^{2+}$. The rate-determining step changes from water displacement to ring-closure to form the tridentate species.

There are a few reports on the X-ray structure of iron(III) complex with pyridoxal isonicotinoyl hydrazone[42,49], the compound of almost the same structure as PBH and PSH. From the X-ray structure of Fe(III)-PIH, PIH acts as a neutral, planar, tridentate ligand and the structure indicates that the ligating sites coordinated to the Fe(III) are the carbonyl oxygen, the imine nitrogen and the phenoxy group of the pyridoxal ring.

The complex is quite very stable in that the 5- and 6- membered ring are formed.

SUMMARY

Pyridoxal Salicyloyl Hydrazone was synthesized and its pK_a were subsequently determined. They are 4.48 (-OH of pyridoxal ring), 7.45 (ring N) and 9.42 (NH-N) respectively. The kinetics of complex formation between $Fe(H_2O)_6^{3+}$ ion and pyridoxal benzoyl hydrazone and pyridoxal salicyloyl hydrazone in aqueous solution have also been measured by conventional spectrophotometry at 25°c, ionic strength of 0.30 M ($NaNO_3$). The measurement was carried out in acid solution (pH not greater than 2.0) to avoid hydrolysis of the ferric ion. The rate constant for the reaction between Fe^{3+} ion and pyridoxal benzoyl hydrazone is 0.52 $M^{-1}s^{-1}$ and for the reaction between $FeOH^{2+}$ and pyridoxal benzoyl hydrazone is 54.57 $M^{-1}s^{-1}$. Also rate constant for the reaction of Fe^{3+} with pyridoxal salicyloyl hydrazone is 0.55 $M^{-1}s^{-1}$ and for the reaction of $FeOH^{2+}$ with pyridoxal salicyloyl hydrazone is 13.64 $M^{-1}s^{-1}$. The rate-determining step is proposed to be ring-closure, on the basis of the low values of the rate constants observed.

APPENDICES

Appendix A

Calculation of Hydrolysis Constant for Fe(III)

From the paper of R.N. Mulburn and W.C. Vosberg[44], it can be seen that the hydrolysis constants are related to the ionic strength by equation ;

$$\log K_{OH} = -2.172-2.040I^{\frac{1}{2}}/ (1 + 2.400I^{\frac{1}{2}})-0.010I$$

where $Fe^{3+} + H_2O \rightleftharpoons FeOH^{2+} + H^+$

$$K_{OH} = \frac{[FeOH^{2+}][H^+]}{[Fe^{3+}]}$$

For I = 0.30 M, $K_{OH} = 2.199 \times 10^{-3}$ M.

REFERENCES

1. B. Modell, Prog. Hematol., 9, 232(1979).
2. P. Ponka, J. Borova, J. Neuwirt and O. Fuchs, FEBS Letters, 97, 317(1979).
3. D.K. Johnson, M.J. Pippard, T.B. Murphy and N.J. Rose, J. Pharmacol. Exp. Ther., 221, 399(1982).
4. M. Gallego, M. Valcarcel and M. Garcia-Vargas, Anal. Chim. Acta., 138, 311(1982).
5. M. Gallego, M. Valcarcel and M. Garcia-Vargas, Analyst., 108, 93(1983).
6. H.S. Frank and W.-Y. Wen, Disc. Faraday. Soc., 24, 133(1957); G. Nemethy and H.A. Scheraga, J. Chem. Phys., 36, 3382(1962).
7. B.G. Cox, G.R. Hedwig, A.J. Parker and D.W. Watts, Aust. J. Chem., 27, 477(1974).
8. J. Burgess, "Metal Ions in Solution", John Wiley & Sons, New York, 1978.
9. R.M. Hol[illegible]er, C.D. Hubbard, S.F.A. Kettle and R.R. Wilkins, Inorg. Chem., 4, [illegible](1965).
10. R.J. Pe[illegible], J. Amer. Chem. Soc., 80, 5059(1958).
11. M. Eigen, Z. Phys. Chem. (Frankfurt.), 1, 176(1954).
12. D.B. Rorabacher and C.A. Melendez-Cepeda, J. Amer. Chem. Soc., 93, 6071(1971).
13. K. Kustin, R.F. Pasternack and E.M. Weinstock, J. Amer. Chem. Soc., 88, 4610(1968).
14. A. Kowalak, K. Kustin, R.F. Pasternack and S. Petrucci, J. Amer. Chem. Soc., 89, 3126(1967).
15. M.B. Makinen, A.F. Pearlmutter and J.E. Stuehr,

J. Amer. Chem. Soc., 91, 4085(1969).

16. R.E. Connick and E.D. Stover, J. Phys. Chem., 65, 2075(1961).
17. G. Czerlinski, "Chemical Relaxation", Arnold, London, 1966.
18. R.G. Wilkins, Acc. Chem. Res., 3, 408(1970).
19. F. Secco and M. Venturini, Inorg. Chem., 14, 1978(1975).
20. J.P. Hunt, Coord. Chem. Rev., 7, 1(1971).
21. T.R. Stengle and C.H. Langford, Coord. Chem. Rev., 2, 344(19 (1967).
22. C.H. Langford, Inorg. Nucl. Chem. Letters., 9, 679(1973).
23. G.T. Lin and F.C. Rorabacher, Inorg. Chem., 12, 2402(1973).
24. D. Langmuir, Geol. Surv. Prof. Pap. (U.S.) 1969, No. 650-B ; Chem. Abstr. 1969, 71, 43022s.
25. R.N. Sylva, Rev. Pure Appl. Chem., 22, 115(1972).
26. C.F. Baes, Jr. and R.E. Mesmer, "The Hydrolysis of Cations", Wiley-Interscience, New York, 1976, p. 229-237.
27. R.M. Smith and A.E. Martell, "Critical Stability Constants", Plenum Press, New York, 1976, Vol.4, p. 7.
28. A. Bino and D. Gibson, J. Amer. Chem. Soc., 104, 4383(1982).
29. A. Bino and D. Gibson, Inorg. Chem., 23, 109(1984).
30. C.J. Carrano and S. Spartalin, Inorg. Chem., 14, 1993(1984).
31. R. Arnek and K. Schylter, Acta. Chem. Scan., 22, 1327(1968).
32. M. Eigen and R.G. Wilkins, Advan. Chem. Ser., No.49, 55 (1965) ; see also M. Eigen, Pure. Appl. Chem., 6, 67(1963).
33. H. Wendt, Inorg. Chem., 8, 1527(1969).
34. R.E. Connick and C.P. Coppel, J. Amer. Chem. Soc., 81, 6389 (1959).

35. J.H Espensen and D.F. Dustin, Inorg. Chem., 8, 1760(1969).

36. D. Seewald and N. Sutin, Inorg. Chem., 2, 643(1963).

37. S. Gouger and J. Stuehr, Inorg. Chem., 13, 379(1974).

38. A.I.Vogel, "A Text Book of Quantitative Inorganic Analysis", 3nd ed. Longman, London, 1961.

39. S. Archer and M.M. Auerbach, Chem. Abstr., 1957, 51, 6705F.

40. C. Sangma, M.Sc. Thesis, Faculty of Graduate Studies, Mahidol University, 1984.

41. [illegible], Aust. J. Chem., 16, 772(1963).

42. M.L. Vitolo, Ph.D. Thesis, Loyedock University, 1984.

43. L.G. Sillen, Quart. Revs., 13, 146(1959).

44. R.M. Milburn and W.C. Vosberg, J. Amer. Chem. Soc., 77, 1352 (1955).

45. E. Mentasti, F. Secco and M. Venturini, Inorg. Chem., 21, 602(1982).

46. J.D. Prue, J. Chem. Educ., 46, 12(1969).

47. J.D. Prue, J. Chem. Soc. A., 1331(1965).

48. E. Mentasti, Inorg. Chem., 18, 1512(1979).

49. T.B. Murphy, D.K. Johnson, N.J. Rose and A. Aruffo, Inorg. Chem. Acta., 66, L67(1982).

50. J.C. Cassett and R.G. Wilkins, J. Amer. Chem. Soc., 90, 6045 (1968).

51. T.J. Byadelek and A.H. Constant, Inorg. Chem., 4, 833(1965).

52. T.J. Byadelek and M.L. Blomster, ibid., 3, 667(1964).

53. R.W. Taylor, H.K. Stepien and D.B. Rorabacher, Inorg. Chem., 13, 1282(1974).

54. J.C. Cassett, W.A. Johnson, L.H. Smith and R.G. Wilkins, J. Amer. Chem. Soc., 94, 8399(1972).

55. F. Basolo, R.C. Johnson, "Coordination Chemistry, The Chemistry of Metal Complexes", W.A. Benjamin, New York, 1964.

56. F. Basolo, R.G. Pearson, "Mechanism of Inorganic Reactions", John Wiley & Sons, New York, 1958.

57. R.G. Wilkins, "The Study of Kinetics and Mechanism of Reactions of Transition Metal Complexes", Allyn and Bacon, Boston, 1974.

58. C.H. Langford and V.S. Sastri, "Reaction Mechanism in Inorganic Chemistry", MTP International Review of Science, Inorganic Chemistry, Series One, V.9, Butterworths, London, 1972.

59. R.M. Silverstein, G.G. Bassler and T.C. Morrill, "Spectrometric Identification of Organic Compounds", 4th ed., John Wiley & Sons, New York, 1981.

60. K. A. Szymanski, "Interpreted Infrared Spectra", Plenum Press, New York, 1964.